$\alpha_{\mathrm{QED,\,eff}}(s)$ for precision physics at the FCC-ee/ILC

Fred Jegerlehner

Deutsches Elektronen–Synchrotron (DESY), Platanenallee 6, D–15738 Zeuthen, Germany

Humboldt–Universität zu Berlin, Institut für Physik, Newtonstrasse 15, D–12489 Berlin, Germany

Abstract:

Discovering "Physics behind precision" at future linear or circular colliders (ILC/FCC projects) requires improved SM predictions based on more precise input parameters. I will review the role $\alpha_{\mathrm{QED,\,eff}}(s)$ at future collider energies and report on possible progress based on results from low energy hadron production facilities. I also discuss the non-perturbative hadronic effects in the running of the $SU(2)$ gauge coupling $\alpha_2(s)$ and the weak mixing parameter $\sin^2\Theta_f(s)$.

Contents

1 $\alpha(M_Z^2)$ in precision physics (precision physics limitations)

Uncertainties of hadronic contributions to the effective fine structure constant $\alpha \equiv \alpha_{\text{QED}}$ are a problem for electroweak (EW) precision physics. Presently, we have α, G_μ, M_Z as the most precise input parameters, which together with the top Yukawa y_t and the Higgs self-coupling λ and the strong interaction coupling α_s allow us to make precision predictions for the particle reaction cross sections encompassed by the Standard Model (SM). The cross-section data unfolded form detector and photon radiation resolution effects often are conveniently representable in terms of so-called pseudo-observables like $\sin^2 \Theta_f, v_f, a_f, M_W, \Gamma_Z, \Gamma_W, \cdots$ as illustrated in Fig. 1. Because of the large 6% relative correction between α in the classical limit and the effective value $\alpha(M_Z^2)$ at the Z mass scale, where 50% of the shift is due to non-perturbative hadronic effects, one is loosing about a factor of five orders of magnitude in precision. Nevertheless, for vector-boson Z and W, top-quark and Higgs-boson precision physics possible at future $e^+ e^-$ colliders, the best effective input parameters are given by $\alpha(M_Z), G_\mu, M_Z$. The effective $\alpha(s)$ at a process scale $\sqrt{s}$ is given in terms of the photon vacuum polarization (VP) self-energy correction $\Delta\alpha(s)$ by

$$\alpha(s) = \frac{\alpha}{1 - \Delta\alpha(s)} \ ; \ \ \Delta\alpha(s) = \Delta\alpha_{\text{lep}}(s) + \Delta\alpha_{\text{had}}^{(5)}(s) + \Delta\alpha_{\text{top}}(s) \,. \tag{1}$$

To be included are the perturbative lepton and top-quark contributions in addition to the non-perturbative hadronic VP shift $\Delta\alpha_{\text{had}}^{(5)}(s)$ from the five light quarks and the hadrons they form.

The present accuracies of the corresponding SM input parameter are the following:

$$
\begin{aligned}
\frac{\delta\alpha}{\alpha} &\sim & 3.6 &\times & 10^{-9} \,, \\
\frac{\delta G_\mu}{G_\mu} &\sim & 8.6 &\times & 10^{-6} \,, \\
\frac{\delta M_Z}{M_Z} &\sim & 2.4 &\times & 10^{-5} \,, \\
\frac{\delta\alpha(M_Z)}{\alpha(M_Z)} &\sim & 0.9 \div 1.6 &\times & 10^{-4} & \text{(present : lost } 10^5 \text{ in precision!)} \,, \\
\frac{\delta\alpha(M_Z)}{\alpha(M_Z)} &\sim & 5 &\times & 10^{-5} & \text{(FCC} - \text{ee/ILC requirement)} \,.
\end{aligned}
\tag{2}
$$

We further note that $\frac{\delta M_W}{M_W} \sim 1.5 \times 10^{-4}$, $\frac{\delta M_H}{M_H} \sim 1.3 \times 10^{-3}$, $\frac{\delta M_t}{M_t} \sim 2.3 \times 10^{-3}$, at present. Evidently, $\alpha(s)$ is the least precise among the basic input parameters and requires a major effort of improvement. As an example, one of the most precisely measured derived observable, the leptonic weak mixing parameter $\sin^2 \Theta_{\ell\,\text{eff}} = (1 - v_\ell/a_\ell)/4 = 0.23148 \pm 0.00017$ and also the related W mass $M_W = 80.379 \pm 0.012$ GeV are affected by the present hadronic error $\delta\Delta\alpha(M_Z) = 0.00020$ in predictions by $\delta \sin^2 \Theta_{\ell\,\text{eff}} = 0.00007$ and $\delta M_W/M_W \sim 4.3 \times 10^{-5}$, respectively. These uncertainties affect most future precision tests and may obscure new physics searches! In order to reduce hadronic uncertainties for perturbative QCD (pQCD) contributions, last but not least, it is very crucial also to improve the precision of QCD parameters α_s, m_c, m_b, m_t which is a big challenge also for lattice-QCD.

The relevance of $\alpha(M_Z^2)$

Understanding precisely even the simplest four fermion, vector boson and Higgs boson production and decay processes, requires very precise input parameters. Unlike in QED and QCD in the SM, a Spontaneously Broken non-Abelian Gauge Theory (SBGT), there are intricate parameter inter-dependences, all masses are related to couplings, only 6 quantities (besides $f \neq t$ fermion masses and mixing parameters) α, G_μ, M_Z in addition to the QCD coupling α_s, the top-quark Yukawa coupling y_t and the Higgs boson self-coupling λ_H are independent. The effective $\alpha(M_Z^2)$ exhibits large
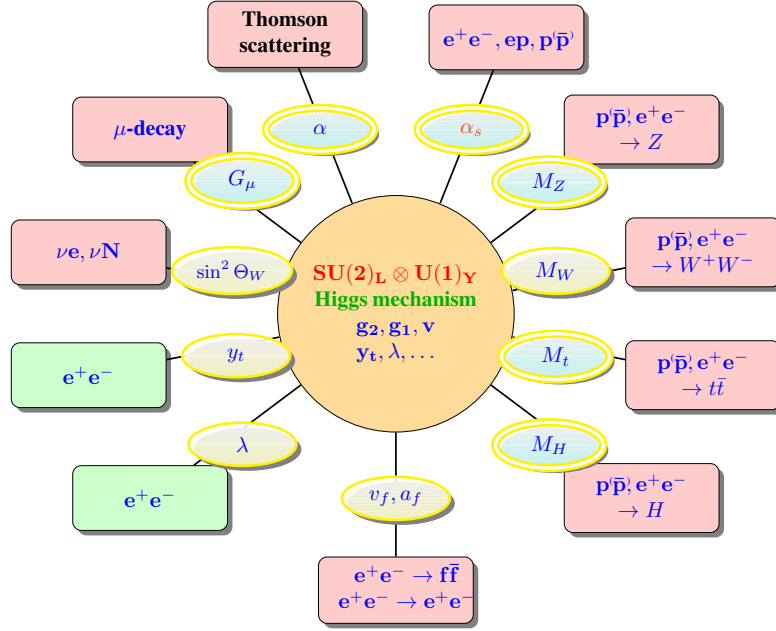
Fig. 1: Many precisely measurable pseudo-observables associated with scattering-, production- and decay processes are interrelated and predictable in terms of a few independent input parameters.

hadronic correction that affect prediction like versions of the weak mixing parameter via

$$\sin^2 \Theta_i \cos^2 \Theta_i \; = \; \frac{\pi \alpha}{\sqrt{2} \, G_\mu \, M_Z^2} \frac{1}{1 - \Delta r_i} \; ; \quad \Delta r_i = \Delta r_i(\alpha, G_\mu, M_Z, m_H, m_{f \neq t}, m_t) \,, \tag{3}$$

with quantum corrections from gauge boson self-energies, vertex- and box- corrections. Δr_i depends on the definition of $\sin^2 \Theta_i$. The various definitions coincide at tree level and hence only differ by quantum effects. From the weak gauge boson masses, the electroweak gauge couplings and the neutral current couplings of the charged fermions we obtain

$$\sin^2 \Theta_W \; = \; 1 - \frac{M_W^2}{M_Z^2} \,, \tag{4}$$

$$\sin^2 \Theta_g \; = \; e^2/g^2 = \frac{\pi \alpha}{\sqrt{2} \, G_\mu \, M_W^2} \,, \tag{5}$$

$$\sin^2 \Theta_f \; = \; \frac{1}{4|Q_f|} \left(1 - \frac{v_f}{a_f} \right) \,, \quad f \neq \nu \,, \tag{6}$$

for the most important cases and the general form of Δr_i reads

$$\Delta r_i \; = \; \Delta \alpha - f_i(\sin^2 \Theta_i) \, \Delta \rho + \Delta r_{i \, \text{reminder}} \,, \tag{7}$$

with a universal term $\Delta \alpha$, which affects the predictions of M_W, A_{LR}, A_{FB}^f, Γ_f, etc. The leading corrections are $\Delta \alpha(M_Z^2) = \Pi_\gamma'(0) - \text{Re}\Pi_\gamma'(M_Z^2)$ from the running fine structure constant and $\Delta \rho = \frac{\Pi_Z(0)}{M_Z^2} - \frac{\Pi_W(0)}{M_W^2} + 2 \frac{\sin \Theta_W}{\cos \Theta_W} \frac{\Pi_{\gamma Z}(0)}{M_Z^2}$, which is proportional to $G_\mu M_t^2$ and therefore large, dominated by the heavy top-quark mass effect, respectively, by the large top Yukawa coupling.

The uncertainty $\delta\Delta\alpha$ implies uncertainties δM_W, $\delta \sin^2 \Theta_i$ given by

$$\frac{\delta M_W}{M_W} \sim \frac{1}{2} \frac{\sin^2 \Theta_W}{\cos^2 \Theta_W - \sin^2 \Theta_W} \delta\Delta\alpha \sim 0.23\, \delta\Delta\alpha\,, \tag{8}$$

$$\frac{\delta \sin^2 \Theta_f}{\sin^2 \Theta_f} \sim \frac{\cos^2 \Theta_f}{\cos^2 \Theta_f - \sin^2 \Theta_f} \delta\Delta\alpha \sim 1.54\, \delta\Delta\alpha\,. \tag{9}$$

Also affected are the important relationships between couplings and masses like

$$\lambda = 3\ \sqrt{2} G_\mu M_H^2 \left(1 + \delta_H(\alpha, \cdots)\right)\,; \quad y_t^2 = 2\ \sqrt{2} G_\mu M_t^2 \left(1 + \delta_t(\alpha, \cdots)\right), \tag{10}$$

which by now offer the only way to determine λ and y_t via the experimentally accessible masses M_H and M_t. The direct measurement of λ and y_t likely will be possible only at future lepton colliders like the FCC-ee.

The parameter relationships between very precisely measurable quantities provide stringent precision tests and at high enough precision would reveal the physics missing within the SM. Presently, the non-perturbative hadronic contribution $\Delta\alpha_{\mathrm{had}}^{(5)}(M_Z^2)$ is limiting the precision predictions. Concerning the relevance of quantum corrections and their precision, one should keep in mind that a 30 SD disagreement between some SM prediction and experiment is obtained when subleading SM corrections are neglected, and only the leading corrections $\Delta\alpha(M_Z^2)$ and $\Delta\rho$ in (7) are accounted for.

2 The ultimate motivation for high precision SM parameters

After the ATLAS and CMS Higgs discovery at the LHC, the Higgs vacuum stability issue is one of the most interesting to be clarified at future e^+e^- facilities. Much more surprising than the discovery of its true existence is the fact that the Higgs boson turned out to exhibit a mass very close to what has been expected from vacuum stability extending up to the Planck scale Λ_{Pl} (see Fig. 2). It looks to be a very tricky conspiracy with other couplings to reach this "purpose". Related is the question of whether the SM allows us to extrapolate it up to Planck scale. So, the central issue for the future is the very delicate "acting together" between SM couplings, which make the precision determination of SM parameters more important than ever. Therefore, higher precise SM parameters g', g, g_s, y_t, λ are mandatory for progress in this direction. Actually, the vacuum stability in controversial at present at the 1.5 σ level between a meta-stable and an stable EW vacuum, which depends on whether λ stays positive up to Λ_{Pl} or not. This is illustrated in Fig. 3. If the SM extrapolates stable to Λ_{Pl}, obviously the resulting effective parameters affect early cosmology, Higgs inflation, Higgs reheating etc. [3]. The sharp dependence of the Higgs vacuum stability on the SM input parameters and on possible SM extensions and the vastly different scenarios that can result as a consequence of minor shifts in parameter space makes the stable vacuum case a particularly interesting one and it could reveal the Higgs particle as "the master of the universe". After all, it is commonly accepted that dark energy provided by some scalar field is the "stuff" shaping the universe both at very early (inflation) as well as at the late times (accelerated expansion).

It is very well conceivable that perturbation expansion works up to the Planck scale without a Landau pole or other singularities and Higgs potential remains (meta)stable! The discovery of the Higgs boson for the first time has supplied us with the complete set of SM parameters and for the peculiar SM configuration, revealed that all SM couplings with the exception of the hypercharge g_1 are decreasing with energy. Very surprisingly, this implies that perturbative SM predictions get the better the higher the energy. More specifically the pattern now looks as follows: the gauge coupling related
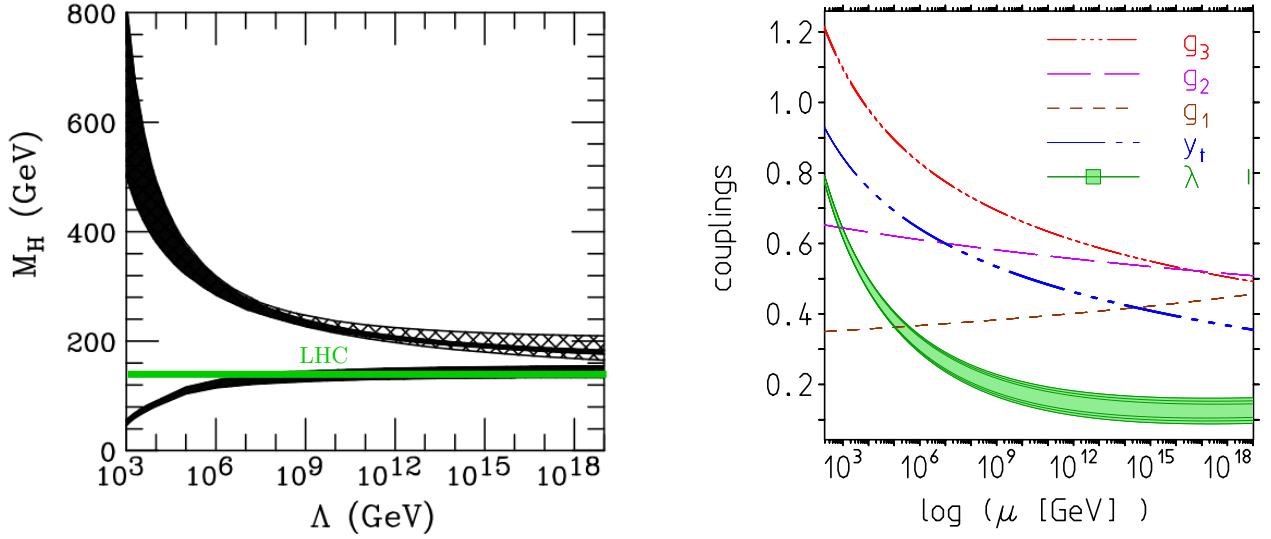
Fig. 2: Left: Plot by Riesselmann and Hambye in 1996, the first 2-loop analysis after knowing M_t from CDF [1]. Right: the SM dimensionless couplings in the $\overline{MS}$ scheme as a function of the renormalization scale for $M_H = 124 - 126\,\text{GeV}$, which were obtained in [2–5].

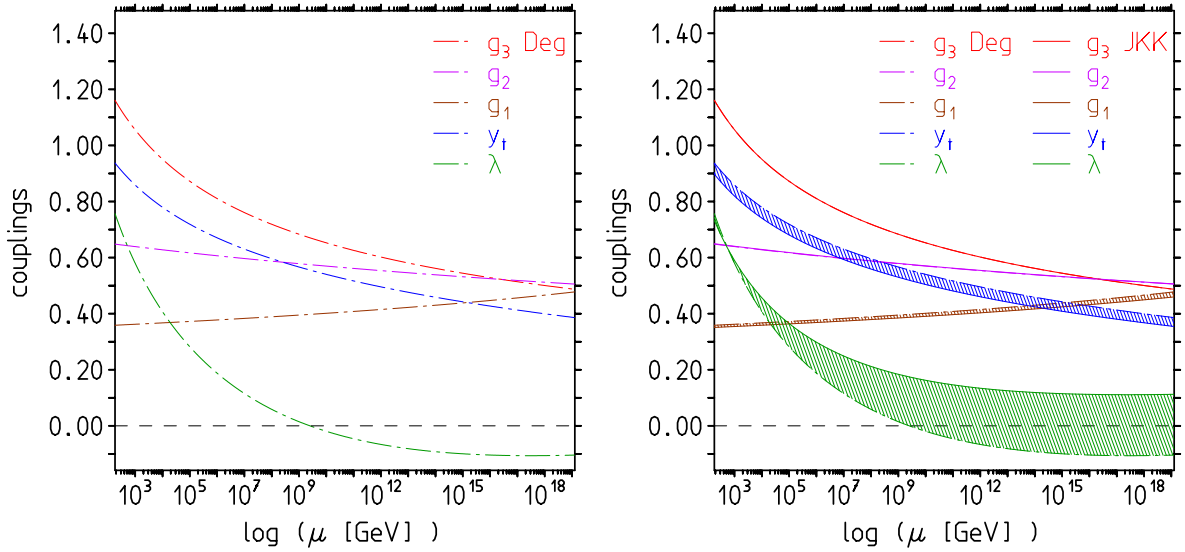

Fig. 3: Left: Shaposhnikov et al., Degrassi et al. matching [6,7]. Right: the shaded bands show the difference in the SM parameter extrapolation using the central values of the $\overline{MS}$ parameters obtained from differences in the matching procedures.

to $U(1)_Y$ is screening (IR free), the ones accociated with $SU(2)_L$ and $SU(3)_c$ are antiscreening (UV free). Thus g_1, g_2, g_3 behave as expected (standard wisdom). In contrast, the top Yukawa coupling y_t and Higgs self-coupling λ, while screening if standalone (IR free, like QED), as part of the SM, they are transmuted from IR free to UV free. The SM reveals an amazing parameter conspiracy, which reminds us of phenomena often observed in condensed matter systems *"... there is a sudden rapid passage to a totally new and more comprehensive type of order or organization, with quite new emergent properties ..."* [8] i.e. there must be reasons that couplings are as they are. This manifests itself in the QCD dominance within the renormalization group (RG) of the top-Yukawa

coupling, which requires $g_3 > \frac{3}{4} y_t$ and in the top-Yukawa dominance within the RG of the Higgs-boson coupling, which requires $\lambda < \frac{3(\sqrt{5}-1)}{2} y_t^2$ in the gaugeless ($g_1, g_2 = 0$) limit. In the focus is the Higgs self-coupling. Does it stay positive $\lambda > 0$ up to Λ_{Pl}? A zero $\lambda = 0$ would be essential singularity. The key question/problem concerns the precise size of the top-Yukawa coupling y_t, which decides about the stability of our world! The meta-stability vs. stability controversy will be decided by getting more precise input parameters and by better established EW matching conditions. Most important in this context is the direct measurements of y_t and λ at future e^+e^--colliders. But also the important role that the running gauge couplings are playing, requires substantial progress in obtaining more precise hadronic cross sections in order to reduce hadronic uncertainties in $\alpha(M_Z)$ and $\alpha_2(M_Z)$. A big challenge for low energy hadron facilities. Complementary, progress in lattice QCD simulations of two-point correlators will be important to pin down hadronic effects from first principles. Such improvement in SM precision physics could open the new gate to precision cosmology of the early universe!

3 R-data evaluation of $\alpha(M_Z^2)$

What we need is a precise calculation of the hadronic photon vacuum polarization function. The non-perturbative hadronic piece from the five light quarks $\Delta\alpha_{\text{had}}^{(5)}(s) = -\left(\Pi_\gamma'(s) - \Pi_\gamma'(0)\right)_{\text{had}}^{(5)}$ can be evaluated in terms of $\sigma(e^+e^- \to \text{hadrons})$ data via the dispersion integral

$$\Delta\alpha_{\text{had}}^{(5)}(s) = -\frac{\alpha\, s}{3\pi} \left(\fint_{m_{\pi_0}^2}^{E_{\text{cut}}^2} ds' \, \frac{R_\gamma^{\text{data}}(s')}{s'(s'-s)} + \fint_{E_{\text{cut}}^2}^{\infty} ds' \, \frac{R_\gamma^{\text{pQCD}}(s')}{s'(s'-s)} \right), \tag{11}$$

where $R_\gamma(s) \equiv \sigma^{(0)}(e^+e^- \to \gamma^* \to \text{hadrons})/\left(\frac{4\pi\alpha^2}{3s}\right)$ measures the hadronic cross-section in units of the tree level $e^+e^- \to \mu^+\mu^-$ cross-section sufficiently above the muon pair production threshold ($s \gg 4m_\mu^2$). The master equation (11) is based on analyticity and the optical theorem

A compilation of the available R-data is shown in Fig. 4 for the low energy $\pi\pi$ channel and in Fig. 5 for $R(s)$ above the ρ resonance peak. Since the mid 90's [54] enormous progress has been achieved, also because the new Initial State Radiation (ISR) radiative return approach[1] provided high statistics data from ϕ- and B-meson factories (see [9–52]). Still, an issue in hadronic vacuum polarization (HVP) is the region 1.2 to 2 GeV, where we have a test-ground for exclusive (more than 30 channels) versus inclusive R measurements, where data taking and/or data analysis is ongoing with CMD-3 and SND detectors [scan] and BaBar and BESIII detector data [radiative return]. The region still contributes about 50% to the uncertainty of the hadronic contribution to the muon $g - 2$, as we may learn from Fig. 8 below. Above 2 GeV fairly accurate BES II data [48–50] are available. Recently, a new inclusive determination of $R_\gamma(s)$ in the range 1.84 to 3.72 GeV has been obtained with the KEDR detector at Novosibirsk [51, 52] (see Fig. 5). At present the results from the direct and the Adler

---

[1]It has been pioneered by the KLOE Collaboration, followed by BaBar and BESIII experiments.
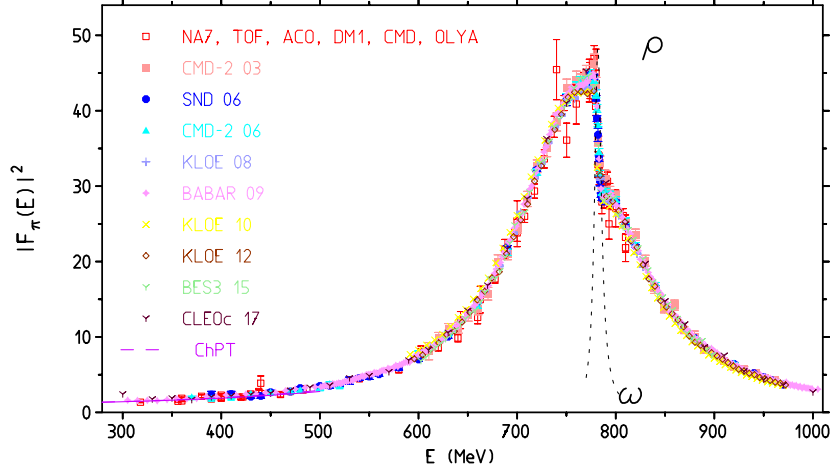
Fig. 4: The low energy tail of R is provided by $\pi^+\pi^-$ production data. Shown is a compilation of the modulus square of the pion form factor in the ρ meson region. The corresponding $R(s)$ is given by $R(s) = \frac{1}{4}\beta_\pi^3 |F_\pi^{(0)}(s)|^2$, $\beta_\pi = (1 - 4m_\pi^2/s)^{1/2}$ is the pion velocity ($s = E^2$). Data from CMD-2, SND, KLOE, BaBar, BESIII and CLEOc [9–23] besides some older sets.
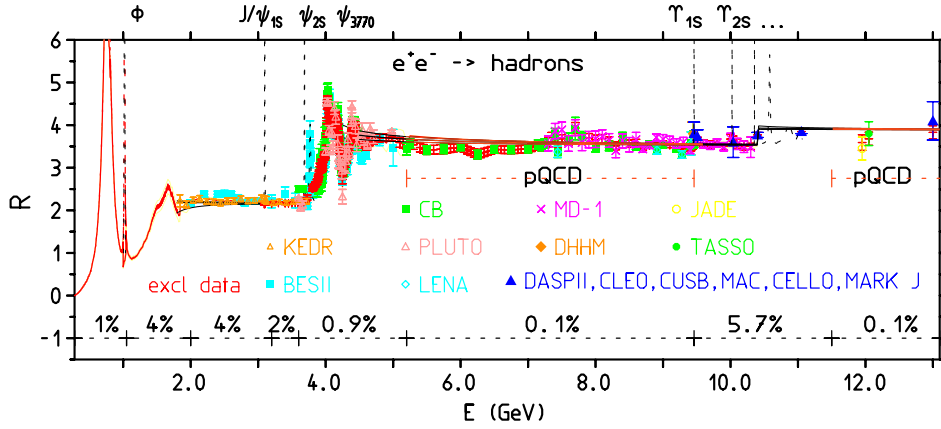

Fig. 5: The compilation of $R(s)$-data utilized in the evaluation of $\Delta\alpha_{\text{had}}$. The bottom line shows the relative systematic errors within the split regions. Different regions are assumed to have uncorrelated systematics. Data from [24–52] and others. We apply pQCD from 5.2 GeV to 9.46 GeV and above 11.5 GeV using the code of [53].

function improved approach to be discussed in Sect. 4 reads

$$
\begin{aligned}
\Delta\alpha_{\text{hadrons}}^{(5)}(M_Z^2) &= 0.027756 \pm 0.000157 \\
&\quad\, 0.027563 \pm 0.000120 \quad \text{Adler} \\
\alpha^{-1}(M_Z^2) &= 128.916 \pm 0.022 \\
&\quad\, 128.953 \pm 0.016 \qquad\quad \text{Adler}
\end{aligned}
\tag{12}
$$

In Fig. 7 we show the effective fine structure constant as a function of the c.m. energy $E = \sqrt{s}$, for the time-like and the space-like region. The question now, what are the possible improvements? Evidently,

• a direct improvement of the dispersion integral requires reducing the error of $R(s)$ to 1% up to above the Υ resonances, likely nobody will do that. One may trust relying on pQCD above 1.8 GeV and
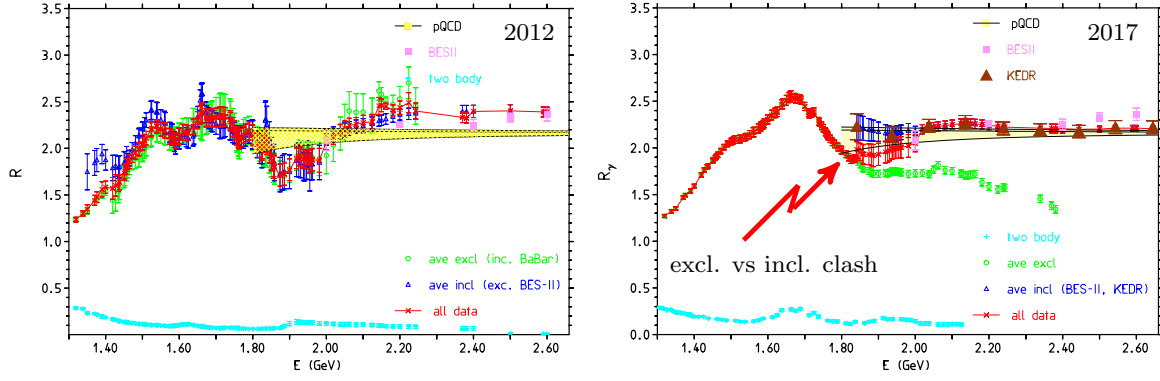
Fig. 6: Illustrating progress by BaBar and NSK exclusive channel data vs. new inclusive data by KEDR. Why point at 1.84 GeV so high?

refer to quark-hadron duality as in [55]. Then experimental input above 1.8 GeV is not required. But then we are left with questions about where precisely to assume thresholds and what are the mass effects near thresholds. Commonly, pQCD is applied taking into account uncertainties in α_s only. This certainly does not provide a result that can be fully trusted, although the R-data integral in this range is much less precise at present. The problem is that in this theory-driven approach 70% of $\Delta\alpha_{\text{had}}^{(5)}(M_Z^2)$ comes from pQCD. Thereby one has to assume that in the time-like region above 1.8 GeV pQCD in average works as precise as the usually adopted $\overline{\text{MS}}$ parametrization suggests. Locally, pQCD does not work near thresholds and resonances obviously.

The more promising approach discussed in the following relies on the

• Euclidean split method (Adler-function controlled pQCD), which only requires improved R measurements in the exclusive region from 1 to 2 GeV. Here NSK, BESIII, and Belle II can top what BaBar has achieved. However, in this rearrangement, as important is a substantially more precise calculation of the pQCD Adler-function. Required is an essentially exact massive 4-loop result, which is equivalent to sufficiently high order low- and high-energy expansions, of which a few terms are available already (see [56]).

Because of the high sensitivity to the precise charm and bottom quark values one also needs better parameters m_c and m_b besides α_s. Here one can profit from activities going on anyway and the FCC-ee/ILC projects pose further strong motivation to attempt to reach higher precision for QCD parameters.

$\Delta\alpha_{\text{had}}(M_Z^2)$ results from ranges

Table 1 shows the contributions and errors to $\Delta\alpha_{\text{had}}^{(5)}(M_Z)$ for $M_Z = 91.1876$ GeV in units 10^{-4} from different regions. Typically, depending on cuts applied the direct evaluation of the dispersion integral of R yields 43% from data and 57% from perturbative QCD. Here, pQCD is used between 5.2 GeV and 9.5 GeV and above 11.5 GeV. Systematic errors are taken correlated within the different ranges, but taken as independent between the different ranges.

In Fig. 8 we illustrate the relevance of different energy ranges by comparing the hadronic contribution to the muon $g - 2$ with the one to the hadronic shift of the effective charge at M_Z. The point is that the new muon $g - 2$ experiments strongly motivate efforts the measure $R(s)$ in the low energy region more precisely. From Fig. 8 we learn that low energy data alone are not able to sub-
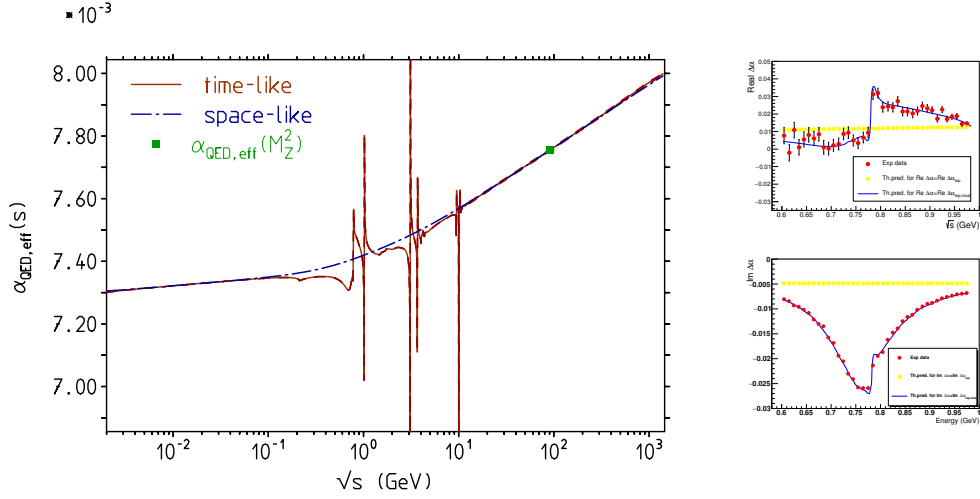
Fig. 7: Left: the effective $\alpha(s)$ at time-like vs. space-like momentum transfer, showing quark-hadron duality at work. In the time-like region, the effective charge is varying dramatically near resonances but agrees quite well on average with the space-like version. Locally, it is ill-defined near OZI suppressed meson decays $J/\psi, \psi_1, \Upsilon_{1,2,3}$ where Dyson series of self-energy insertions do not converge (see Sect. 5 of [57]). Right: a first experimental determination of the effective charge in the ρ resonance region by KLOE-2 [58], which demonstrates the pronounced variation of the vacuum polarization (charge screening) across a resonance.

stantially improve a direct evaluation of the dispersion integral (11). Therefore, in order to achieve the required factor 5 improvement alternative methods to determine $\Delta\alpha_{\text{had}}^{(5)}(s)$ at high energies have to be developed.

4 Reducing uncertainties via the Euclidean split trick: Adler function controlled pQCD

As we learn from Fig. 5 it is difficult if not impossible to tell at what precision pQCD can replace data. This especially concerns resonance and threshold effects and to what extent quark-hadron duality can be made precise. This is much simpler to accommodate by comparison in the Euclidean (space-like) region, as it has been suggested by Adler [59] long time ago and has been successfully tested in [60]. As the data pool has been improving a lot since the "experimental" Adler-function is known with remarkable precision by now. Actually, on the experiment side new more precise measurements of $R(s)$ are going on primarily in the low energy range. On the theory side, pQCD calculations for Euclidean two-point current correlators are expected to be pushed further. Advance is also expected from lattice QCD, which also can produce data for the Adler function. As suggested in [61–63] in the Euclidean region a split into a non-perturbative and a pQCD part is self-evident. One may write

$$\alpha(M_Z^2) = \alpha^{\text{data}}(-M_0^2) + \left[\alpha(-M_Z^2) - \alpha(-M_0^2)\right]^{\text{pQCD}} + \left[\alpha(M_Z^2) - \alpha(-M_Z^2)\right]^{\text{pQCD}}, \tag{13}$$

where the space-like offset M_0 is chosen such that pQCD is well under control for $-s < -M_0^2$. The non-perturbative offset $\alpha^{\text{data}}(-M_0^2)$ may be obtained integrating $R(s)$ data, by choosing $s = -M_0^2$ in (11).

The crucial point is that the contribution from different energy ranges to $\alpha^{\text{data}}(-M_0^2)$ is very different form that to $\alpha^{\text{data}}(M_Z^2)$. Table 1 now is replaced by Table 2 where $\alpha^{\text{data}}(-M_0^2)$ is listed for

Table 1: $\Delta\alpha_{\text{had}}^{(5)}(M_Z)$ in terms of e^+e^--data and pQCD. The last two columns list the relative accuracy and the % contribution of the total. The systematic errors (syst) are assumed to be independent among the different energy ranges listed in the table.

| final state	range (GeV)	$\Delta\alpha_{\text{had}}^{(5)} \times 10^4$ (stat) (syst) [tot]	rel	abs
ρ	(0.28, 1.05)	34.14 (0.03) (0.28)[0.28]	0.8%	3.1%
ω	(0.42, 0.81)	3.10 (0.03) (0.06)[0.07]	2.1%	0.2%
ϕ	(1.00, 1.04)	4.76 (0.04) (0.05)[0.06]	1.4%	0.2%
J/ψ		12.38 (0.60) (0.67)[0.90]	7.2%	31.9%
Υ		1.30 (0.05) (0.07)[0.09]	6.9%	0.3%
had	(1.05, 2.00)	16.91 (0.04) (0.82)[0.82]	4.9%	26.7%
had	(2.00, 3.20)	15.34 (0.08) (0.61)[0.62]	4.0%	15.1%
had	(3.20, 3.60)	4.98 (0.03) (0.09)[0.10]	1.9%	0.4%
had	(3.60, 5.20)	16.84 (0.12) (0.21)[0.25]	0.0%	2.4%
pQCD	(5.20, 9.46)	33.84 (0.12) (0.25)[0.03]	0.1%	0.0%
had	(9.46,11.50)	11.12 (0.07) (0.69)[0.69]	6.2%	19.1%
pQCD	(11.50, 0.00)	123.29 (0.00) (0.05)[0.05]	0.0%	0.1%
data	(0.3,∞)	120.85 (0.63) (1.46)[1.58]	1.0%	0.0%
total		277.99 (0.63) (1.46)[1.59]	0.6%	100.0%
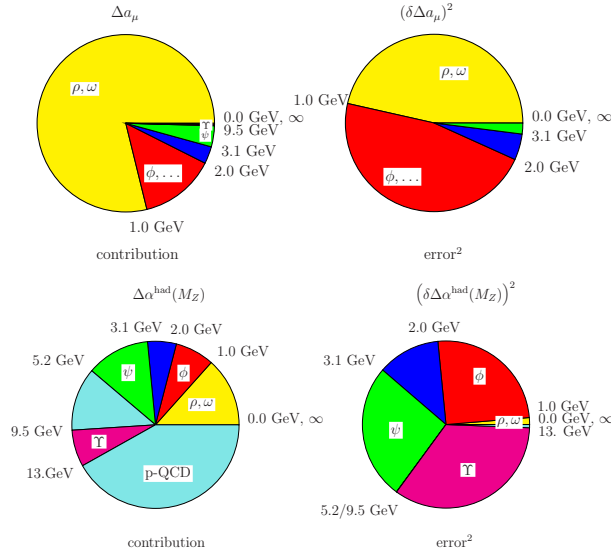
Fig. 8: A comparison of the weights and square uncertainties between a_μ^{had} and $\Delta\alpha_{\text{had}}^{(5)}(M_Z^2)$ of contributions from different regions. It reveals the importance of the different energy regions. In contrast to the low energy dominated a_μ^{had}, $\Delta\alpha_{\text{had}}^{(5)}(M_Z^2)$ is sensitive to data from much higher energies.

$M_0 = 2$ GeV in units 10^{-4}. Here 94% results using data and only 6% pQCD, applied again between 5.2 GeV and 9.5 GeV and above 11.5 GeV. Of $\Delta\alpha_{\text{had}}^{(5)}(M_Z^2)$ 22% data, 78% pQCD! The split point M_0 may be shifted to optimize the uncertainty contributed from the pQCD part and the data based offset value. A reliable estimate of the latter is mandatory and we also have crosschecked its evaluation using the phenomenological effective Lagrangian global fit approach [64, 65], specifically, within the broken Hidden Local Symmetry (BHLS) implementation.

In Fig. 9 we illustrate the relevance of different energy ranges by comparing the hadronic shift

Table 2: $\Delta\alpha_{\text{had}}^{(5)}(-M_0^2)$ at $M_0 = 2$ GeV in terms of e^+e^--data and pQCD. Labels as in Table 1

| final state	range (GeV)	$\Delta\alpha_{\text{had}}^{(5)}(-M_0^2) \times 10^4$ (stat) (syst) [tot]	rel	abs
ρ	(0.28, 1.05)	29.97 (0.03) (0.24)[0.24]	0.8%	14.3%
ω	(0.42, 0.81)	2.69 (0.02) (0.05)[0.06]	2.1%	0.8%
ϕ	(1.00, 1.04)	3.78 (0.03) (0.04)[0.05]	1.4%	0.6%
J/ψ		3.21 (0.15) (0.15)[0.21]	6.7%	11.2%
Υ		0.05 (0.00) (0.00)[0.00]	6.8%	0.0%
had	(1.05, 2.00)	10.56 (0.02) (0.48)[0.48]	4.6%	56.9%
had	(2.00, 3.20)	6.06 (0.03) (0.25)[0.25]	4.2%	15.7%
had	(3.20, 3.60)	1.31 (0.01) (0.02)[0.03]	1.9%	0.2%
had	(3.60, 5.20)	2.90 (0.02) (0.02)[0.03]	0.0%	0.2%
pQCD	(5.20, 9.46)	2.66 (0.02) (0.02)[0.00]	0.1%	0.0%
had	(9.46,11.50)	0.39 (0.00) (0.02)[0.02]	5.7%	0.1%
pQCD	(11.50, 0.00)	0.90 (0.00) (0.00)[0.00]	0.0%	0.0%
data	(0.3,∞)	60.92 (0.16) (0.62)[0.64]	1.0%	0.0%
total		64.47 (0.16) (0.62)[0.64]	1.0%	100.0%
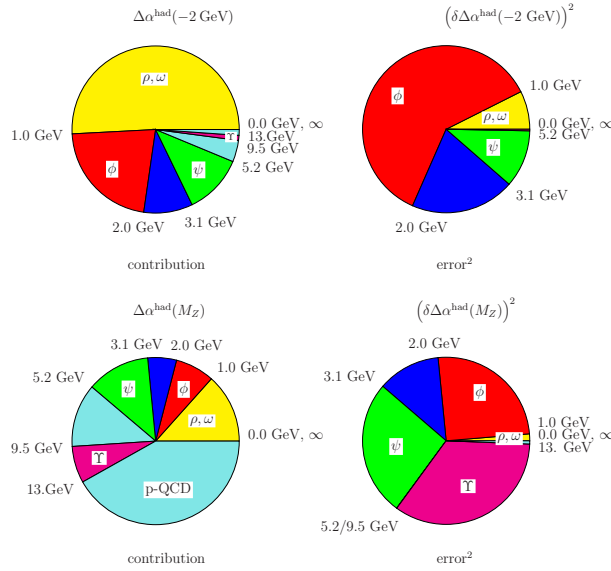
Fig. 9: Contributions and square errors from e^+e^- data ranges and form pQCD to $\Delta\alpha_{\text{had}}^{(5)}(-M_0^2)$ vs. $\Delta\alpha_{\text{had}}^{(5)}(M_Z^2)$.

of the effective charge as evaluated at s space-like low energy scale $M_0 = 2$ GeV with the ones at the time-like M_Z scale. The crucial point is that the profile of the offset α at M_0 much more resembles the profile found for the hadronic contribution to a_μ and improving a_μ^{had} automatically lead to an improvement of $\Delta\alpha_{\text{had}}^{(5)}(-M_0^2)$, this is the profit gained from the Euclidean split trick.

What does this have to do with the Adler function? The Adler function is **i)** the monitor to control the applicability of pQCD and **ii)** the pQCD part $\left[\alpha(-M_Z^2) - \alpha(-M_0^2)\right]^{\text{pQCD}}$ is favorably calculated by integrating the Adler function $D(Q^2)$. The small remainder $\left[\alpha(M_Z^2) - \alpha(-M_Z^2)\right]^{\text{pQCD}}$ can be obtained in terms of the VP function $\Pi'_\gamma(s)$. In fact, the Adler function is the ideal monitor for

comparing theory and data. The Adler function is defined as the derivative of the VP function:

$$D(-s) \doteq \frac{3\pi}{\alpha} \, s \, \frac{\mathrm{d}}{\mathrm{d}s} \Delta\alpha_{\mathrm{had}}(s) = -\left(12\pi^2\right) \, s \, \frac{\mathrm{d}\Pi'_\gamma(s)}{\mathrm{d}s} \tag{14}$$

and can be evaluated in terms of e^+e^--annihilation data by the dispersion integral

$$D(Q^2) = Q^2 \left(\int_{4m_\pi^2}^{E_{\mathrm{cut}}^2} \mathrm{d}s \, \frac{R(s)^{\mathrm{data}}}{\left(s + Q^2\right)^2} + \int_{E_{\mathrm{cut}}^2}^{\infty} \mathrm{d}s \, \frac{R^{\mathrm{pQCD}}(s)}{(s + Q^2)^2} \right). \tag{15}$$

It is a finite object not subject to renormalization and it tends to a constant in the high energies limit, where it is perfectly perturbative. Comparing the direct $R(s)$-based and the $D(Q^2)$-based methods

pQCD $\leftrightarrow R(s)$	pQCD $\leftrightarrow D(Q^2)$
very difficult to obtain in theory	smooth simple function in Euclidean region

we note that in time-like approach pQCD only works well in "perturbative windows" roughly in ranges 3.00 - 3.73 GeV, 5.00 - 10.52 GeV and 11.50 GeV - ∞ (see [53]), while in the space-like approach pQCD works well for $Q > 2.0$ GeV, a clear advantage.

In Fig. 10 the "experimental" Adler–function is confronted with theory (pQCD + NP). Note that in contrast to most xfR-plots, like Fig. 5, showing statistical errors only in Fig. 10 the total error is displayed as the shaded band. We see that while 1-loop and 2-loop predictions fail clearly to follow the data band, a full massive 3-loop QCD prediction in the gauge invariant background field MOM scheme [66] reproduces the experimental Adler function surprisingly well. This has been worked out in [60] by Padé improvement of the moment expansions provided in [67–69]. The figure also shows that non-perturbative (NP) contributions from the quark and gluon condensates [70,71][2] start to contribute substantially only at energies where pQCD fails to converge because one is approaching the Landau pole in $\overline{\mathrm{MS}}$ parametrized QCD. Strong coupling constant freezing as in analytic perturbation theory (APT) advocated in [72] or similar schemes actually are not able to improve the agreement in the low energy regime. Coupling constant freezing also contradicts lattice QCD results [73].

From the three terms of (13) we already know the low energy offset $\Delta\alpha_{\mathrm{had}}(-M_0^2)$ for $M_0 = 2.0$ GeV. The second term we obtain by integrating the pQCD predicted Adler function

$$\Delta_1 = \Delta\alpha_{\mathrm{had}}(-M_Z^2) - \Delta\alpha_{\mathrm{had}}(-M_0^2) = \frac{\alpha}{3\pi} \int_{M_0^2}^{M_Z^2} \mathrm{d}Q'^2 \, \frac{D(Q'^2)}{Q'^2}, \tag{16}$$

based on a complete 3-loop massive QCD analysis. The QCD parameters used are $\alpha_s(M_Z) = 0.1189(20)$, $m_c(m_c) = 1.286(13)[M_c = 1.666(17)]$GeV, $m_b(m_c) = 4.164(25)[M_b = 4.800(29)]$GeV. The result obtained is

$$\Delta_1 = \Delta\alpha_{\mathrm{had}}(-M_Z^2) - \Delta\alpha_{\mathrm{had}}(-M_0^2) = 0.021074 \pm 0.000100 .$$

This includes a shift +0.000008 from the massless 4-loop contribution included in the high energy tail. The error ±0.000100 will be added in quadrature. Up to three-loops all contributions have the same sign and are substantial. Four- and higher-orders could still add up to non-negligible contribution. An error for missing higher order terms is not included.

---

[2]These are evaluated by means of operator product expansions and the explicit expressions may be found in [60].
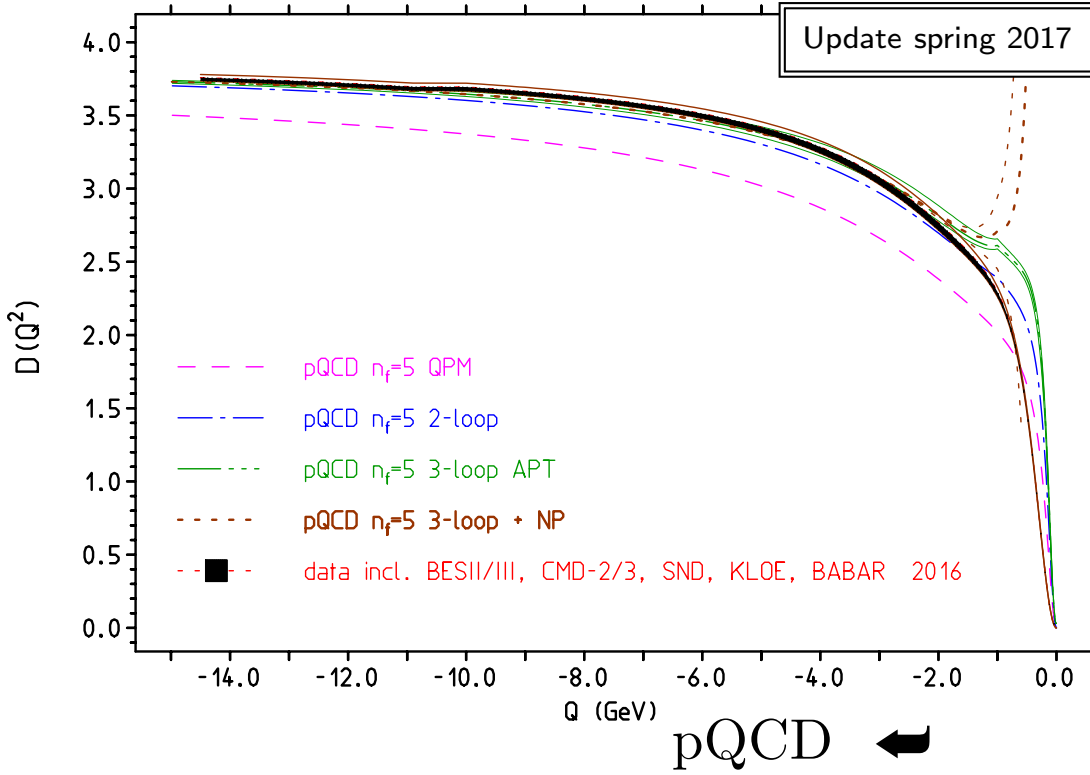
Fig. 10: Monitoring pQCD vs. data: the pQCD prediction of $D(Q^2)$ works well down to $M_0 = 2.0\,\text{GeV}$, provided full massive QCD at 3- or higher-loop order is employed.

The remaining term concerns the link between the space-like and the time-like region at the Z boson mass scale and is given by the difference

$$\Delta_2 = \Delta\alpha_{\text{had}}^{(5)}(M_Z^2) - \Delta\alpha_{\text{had}}^{(5)}(-M_Z^2) = 0.000045 \pm 0.000002\,,$$

which can be calculated in pQCD. It accounts for the $i\pi$-terms from the logs $\ln(-q^2/\mu^2) = \ln(|q^2/\mu^2|) + i\pi$. Since the term is small we can get it as well from direct data integration based on our data compilation. We obtain $\Delta\alpha_{\text{had}}(-M_Z^2) = 276.44 \pm 0.64 \pm 1.78$ and $\Delta\alpha_{\text{had}}(+M_Z^2) = 276.84 \pm 0.64 \pm 1.90$, and taking into account that errors are almost 100% correlated we have $\Delta\alpha_{\text{had}}(M_Z^2) - \Delta\alpha_{\text{had}}(-M_Z^2) = 0.40 \pm 0.12$ less precise but in agreement with the pQCD result. We then have

$$\begin{aligned}
\Delta\alpha_{\text{had}}^{(5)}(-M_0^2)^{\text{data}} &= 0.006409 \pm 0.000063 \\
\Delta\alpha_{\text{had}}^{(5)}(-M_Z^2) &= 0.027483 \pm 0.000118 \\
\Delta\alpha_{\text{had}}^{(5)}(M_Z^2) &= 0.027523 \pm 0.000119 \quad .
\end{aligned}$$

In order to get $\alpha^{-1}(M_Z^2)$ we have to include also the leptonic piece [74]

$$\Delta\alpha_{\text{lep}}(M_Z^2) \simeq 0.031419187418\,, \tag{17}$$

and the top-quark contribution. A very heavy top-quark decouples like

$$\Delta\alpha_{\text{top}} \simeq -\frac{\alpha}{3\pi}\frac{4}{15}\frac{s}{m_t^2} \to 0$$

14

when $m_t \gg s$. At $s = M_Z^2$, the top-quark contributes

$$\Delta\alpha_{\text{top}}(M_Z^2) = -0.76 \times 10^{-4} \quad . \tag{18}$$

Collecting terms, this leads to the result presented in (12) above. One should note that the Adler
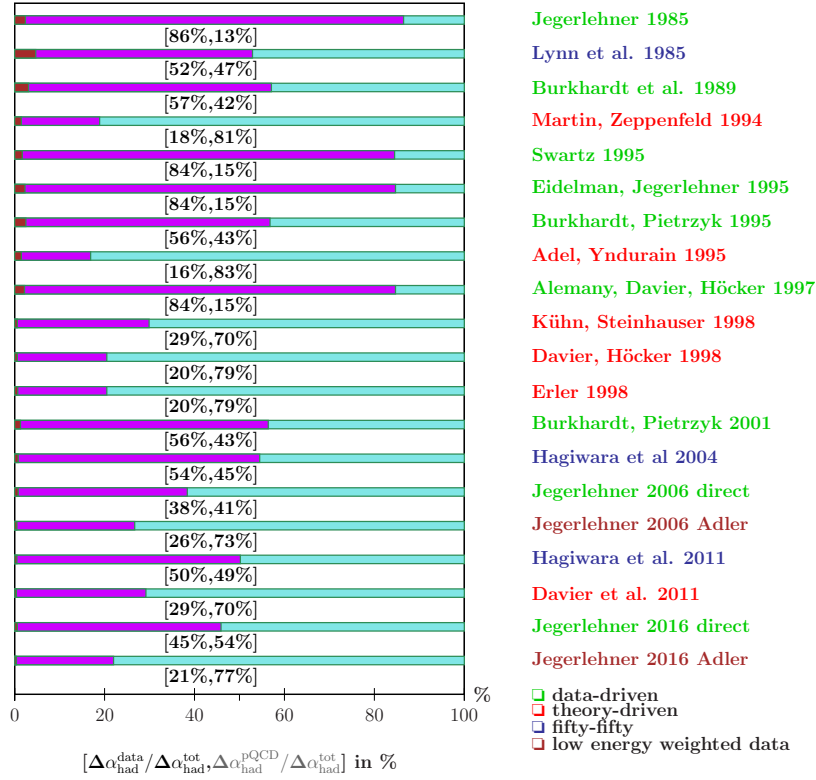

Fig. 11: How much pQCD? Here a history of results by different authors. It shows that the Adler-function controlled approach to $\Delta\alpha_{\text{had}}^{(5)}(M_Z^2)$ is barely more pQCD driven than many of the standard evaluations. The pQCD piece is 70% in Davier et al. [55] and 77% in our Adler-driven case. With an important difference: in the Adler controlled case, the major part of 71% is based on pQCD in the space-like region and only 6% contributing to the non-perturbative offset value is evaluated in the time-like region, while in the standard theory-driven as well as in the more data-driven approaches pQCD is applied in the time-like region, where it is much harder to be tested against data.

function controlled Euclidean data vs. pQCD split approach is only moderately more pQCD-driven, than the time-like approach adopted by Davier et al. [55] and others as follows from the collection of results shown in Fig. 11. The point is that the Adler function driven method only uses pQCD where reliable predictions are possible and direct cross checks against lattice QCD data may be carried out. Similarly, possible future direct measurements of $\alpha(-Q^2)$ in μ-e scattering [75] can provide Euclidean HVP data, in particular also for the offset $\Delta\alpha_{\text{had}}(-M_0^2)$.

5 Prospects for future improvements

The new muon $g - 2$ experiments at Fermilab and at JPARC in Japan (expected to go into operation later) trigger the continuation of $e^+e^- \to$ hadrons cross section measurements in the low energy region by CMD-3 and SND at BINP Novosibirsk, by BES III at IHEP Beijing and soon by Belle II at KEK

Tsukuba. This automatically helps to improve $\Delta\alpha(-M_0^2)$ and hence $\alpha(M_Z^2)$ via the Adler function controlled split-trick approach. As important are the results from lattice QCD, which come closer to be competitive with the data-driven dispersive method.

The improvement by a factor 5 to 10 in this case largely relies on improving the QCD prediction of the two-point vector correlator above the 2 GeV scale, which is a well defined comparably simple task. The mandatory pQCD improvements required are:

- 4-loop massive pQCD calculation of Adler function. In practice, this requires the calculation of a sufficient number of terms in the low- and high-momentum series expansions, such that an accurate Padé improvement is possible.

- m_c, m_b improvements by sum rule and/or lattice QCD evaluations.

- improved α_s in low Q^2 region above the τ mass.

Note that the direct dispersion relations (DR) approach requires precise data up to much higher energies or a heavy reliance on the pQCD calculation of the time-like $R(s)$! The virtues of Adler-function approach are obvious:

- no problems with physical threshold and resonances,
- pQCD is used only where we can check it to work accurately (Euclidean $Q \gtrsim 2.0$ GeV),
- no manipulation of data, no assumptions about global or local duality,
- the non-perturbative "remainder" $\Delta\alpha(-M_0^2)$ is mainly sensitive to low energy data,
- $\Delta\alpha(-M_0^2)$ would be directly accessible in a MUonE experiment (project) [75] or in lattice QCD.

In the direct approach e.g. Davier et al. [55] use pQCD above 1.8 GeV, which means that no error reduction follows from remeasuring cross-sections above 1.8 GeV. Also there is no proof that pQCD is valid at 0.04% precision as adopted. This is a general problem when utilizing pQCD at time-like momenta exhibiting non-perturbative features.

What we can achieve is illustrated in Fig. 12 and the following tabular on the precision in $\alpha(M_Z^2)$:

present	direct	1.7×10^{-4}	
	Adler	1.2×10^{-4}	
future	Adler QCD 0.2%	5.4×10^{-5}	
	Adler QCD 0.1%	3.9×10^{-5}	
future	via $A_{\rm FB}^{\mu\mu}$ off Z	$3 \ \times 10^{-5}$	[78] .

Our analysis shows that the Adler function inspired method is competitive with Patrick Janot's [78] direct near Z pole determination via a measurement of the forward backward asymmetry $A_{\rm FB}^{\mu\mu}$ in $e^+e^- \to \mu^+\mu^-$. The modulus square of the sum of the two tree level diagrams has three terms: the Z-exchange alone $\mathcal{Z} \propto (M_Z^2 G_\mu)^2$, the $\gamma - Z$ interference $\mathcal{I} \propto \alpha(s) M_Z^2 G_\mu$ and the γ-exchange only $\mathcal{G} \propto \alpha^2(s)$. The interference term determines the forward-backward (FB) asymmetry, which is linear in $\alpha(s)$. v denotes the vector $Z\mu\mu$ coupling that depends on $\sin^2\Theta_{\ell\,{\rm eff}}(s)$, while a denotes the axial $Z\mu\mu$ coupling that is sensitive to ρ-parameter (strong M_t dependence). In extracting $\alpha(M_Z^2)$ one is using the v and a couplings as measured at Z-peak directly. At tree level one then has

$$A_{\rm FB}^{\mu\mu} = A_{\rm FB,0}^{\mu\mu} + \frac{3\,a^2}{4\,v^2}\,\frac{\mathcal{I}}{\mathcal{Z} + \mathcal{G}}\;;\;\; A_{\rm FB,0}^{\mu\mu} = \frac{3}{4}\,\frac{4v^2a^2}{(v^2 + a^2)^2}\,, \tag{19}$$
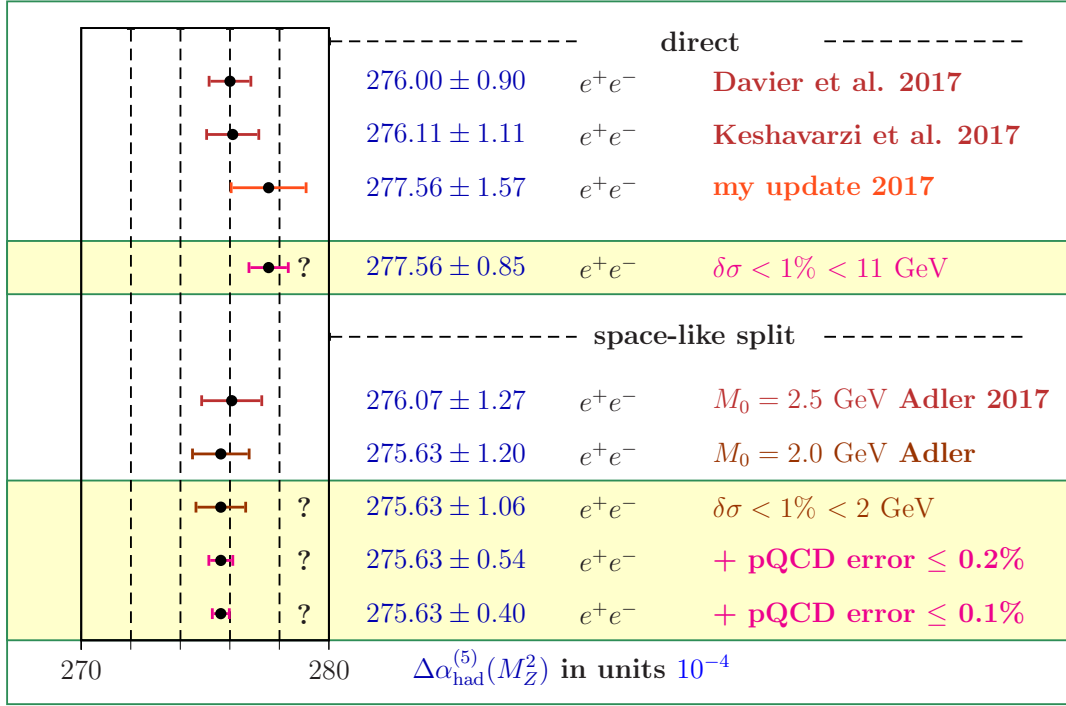
Fig. 12: Comparison of possible improvements. My "direct" analysis is data-driven adopting pQCD in window $5.2-9.5$ GeV and above 11.5 GeV. The Adler-driven results under "space-like split" show the present status for the two offset energies $M_0 = 2.5$ GeV and 2 GeV. The improvement potential is displayed for 3 options: reducing the error of the data offset by a factor two, improving pQCD to a 0.2% precision Adler-function in addition and the same by improving pQCD to a 0.1% precision Adler-function. The direct results are from Refs. [55, 76, 77].

where

$$\mathcal{G} = \frac{c_\gamma^2}{s} \, , \quad \mathcal{I} = \frac{2 c_\gamma c_Z \, v^2 \, (s - M_Z^2)}{(s - M_Z^2)^2 + M_Z^2 \Gamma_Z^2} \, , \quad \mathcal{Z} = \frac{c_Z^2 \, (v^2 + a^2) \, s}{(s - M_Z^2)^2 + M_Z^2 \Gamma_Z^2}$$

$$c_\gamma = \sqrt{\frac{4\pi}{3}} \, \alpha(s) \, , \quad c_Z = \sqrt{\frac{4\pi}{3}} \, \frac{M_Z^2}{2\pi} \, \frac{G_\mu}{\sqrt{2}} \, , \quad v = (1 - 4 \sin^2 \Theta_\ell) \, a \, , \quad a = -\frac{1}{2} \, .$$

Note that $M_Z^2 G_\mu = M_W^2 G_\mu / \cos^2 \Theta_W = \frac{\pi}{\sqrt{2}} \frac{\alpha_2(s)}{\cos^2 \Theta_g(s)}$ and $\sin^2 \Theta_g(s) = \alpha(s)/\alpha_2(s)$. i.e. all parameters vary more or less with energy depending on the renormalization scheme utilized. The challenges for this direct measurement are precise radiative corrections (see [79, 80] and references therein) and requires dedicated off-Z peak running. Short accounts of the methods proposed for improving $\alpha(M_Z^2)$ may be found in Sects. 8 and 9 of [81].

The Adler-function based method is much cheaper to get, I think, and does not depend on understanding the Z peak region with unprecedented precision. Another very crucial point may be that the dispersive method and the Adler-function modified version provide the effective $\alpha(s)$ for arbitrary c.m. energies, not at $s = M_Z^2$ only; although supposed we are given a very precise $\alpha(M_Z^2)$ one can reliably calculate $\alpha(s) - \alpha(M_Z^2)$ via pQCD for s-values in the perturbative regime, i.e. especially when going to higher energies. In any case the requirements specified above to be satisfied in order to reach a factor 5 improvement looks to be achievable.
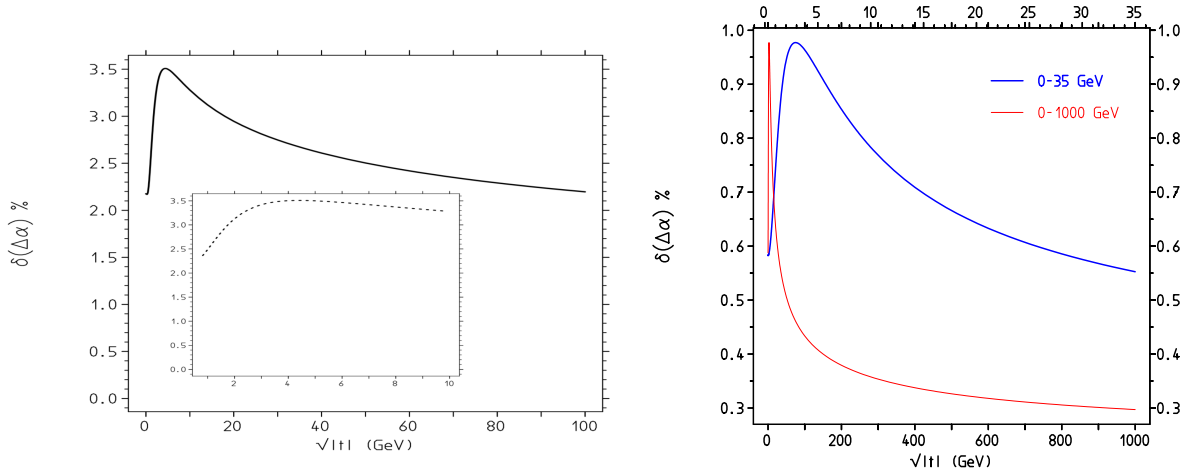
Fig. 13: Hadronic uncertainty $\delta\Delta\alpha_{\text{had}}(\sqrt{t})$. The progress since LEP times 1996 (left) to now (right) is remarkable. Lots of much more precise low energy data $\pi\pi$ etc. are available by now.

6 The need for a space-like effective $\alpha(t)$

As a normalization in measurements of cross-sections in e^+e^- collider experiments, small angle Bhabha scattering is the standard choice. This reference process is dominated by the t-channel diagram of the Bhabha scattering process shown in the left of Fig. 14. In small angle Bhabha scattering
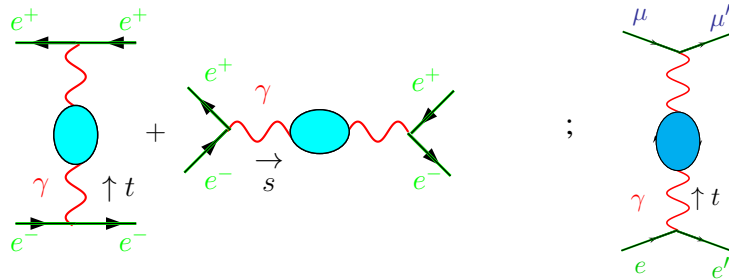

Fig. 14: t-channel dominated QED processes. Left: VP dressed tree level Bhabha scattering at small scattering angles. Right: the leading VP effect in μe scattering.

we have $\delta_{\text{HVP}}\sigma/\sigma = 2\,\delta\alpha(\bar{t})/\alpha(\bar{t})$, and for the FCC-ee luminometer $\sqrt{\bar{t}} \simeq 3.5$ GeV near Z peak and $\simeq 13$ GeV at 350 GeV [82]. The progress achieved after LEP times is displayed in Fig. 13. What can be achieved for the FCC-ee project is listed in the following tabular:

$\sqrt{s}$	$\sqrt{\bar{t}}$	1996 [83, 84]	present	FCC–ee expected [82]
M_Z	3.5 GeV	0.040%	0.013%	0.6×10^{-4}
350 GeV	13 GeV		1.2×10^{-4}	2.4×10^{-4}

The estimates are based on expected improvements possible for $\Delta\alpha_{\text{had}}(-Q^2)$ in the appropriate energy ranges, centered at $\sqrt{\bar{t}}$.

A new project: measuring directly the low energy $\alpha(t)$

The possible direct measurement of $\Delta\alpha_{\text{had}}(-Q^2)$ follows a very different strategy of evaluating the HVP contribution to the muon $g - 2$. There is no VP subtraction issue, there is no exclusive channel separation and recombination, no issue of combining data from very different experiments and

controlling correlations. Even a 1% level measurement can provide invaluable independent information. The recent proposal [75] to measure $\alpha(-Q^2)$ via $\mu^- e^-$-scattering (see right part of Fig. 13) in the `MUonE` projects at CERN is very important for future precision physics. It is based on a cross section measurement

$$\frac{d\sigma^{\text{unpol.}}_{\mu^- e^- \to \mu^- e^-}}{dt} = 4\pi\,\alpha(t)^2\,\frac{1}{\lambda(s,m_e^2,m_\mu^2)}\left\{\frac{\left(s-m_\mu^2-m_e^2\right)^2}{t^2} + \frac{s}{t} + \frac{1}{2}\right\}\,. \tag{20}$$

The primary goal of the project concerns the determination of a_μ^{had} in an alternative way

$$a_\mu^{\text{had}} = \frac{\alpha}{\pi}\int\limits_0^1 dx\,(1-x)\,\Delta\alpha_{\text{had}}\left(-Q^2(x)\right)\,, \tag{21}$$

where $Q^2(x) \equiv \frac{x^2}{1-x}m_\mu^2$ is the space-like square momentum-transfer and

$$\Delta\alpha_{\text{had}}(-Q^2) = \frac{\alpha}{\alpha(-Q^2)} + \Delta\alpha_{\text{lep}}(-Q^2) - 1 \tag{22}$$

directly compares with lattice QCD data and the offset $\alpha(-M_0^2)$ discussed before. We propose to determine very accurately $\Delta\alpha_{\text{had}}\left(-Q^2\right)$ at $Q \approx 2.5\text{GeV}$ by this method (one single number!) as the non-perturbative part of $\Delta\alpha_{\text{had}}\left(M_Z^2\right)$ as needed in the "Adler-function approach". It also would be of direct use for a precise small angle Bhabha luminometer! Because of the high precision required accurate radiative corrections are mandatory and corresponding calculations are in progress [85–88].

7 Conclusions

Reducing the muon $g-2$ prediction uncertainty remains the key issue of high precision physics and strongly motivates more precise measurements of low energy $e^+e^- \to$ hadrons cross sections. Progress is expected from Novosibirsk (VEPP 2000/CMD3,SND), Beijing (BEPCII/BESIII) and Tsukuba (SuperKEKB/BelleII). This helps to improve $\alpha(t)$ in the region relevant for small angle Bhabha scattering and in calculating $\alpha(s)$ at FCC-ee/ILC energies via the Euclidean split-trick method. The latter method requires pQCD prediction of the Adler-function to improve by a factor 2. This also means that we need improved parameters, in particular, m_c and m_b.

One question remains to be asked: Are presently estimated and essentially agreed-on evaluations of $\Delta\alpha_{\text{had}}^{(5)}(M_Z^2)$ in terms of R-data reliable? One has to keep in mind that the handling of systematic errors is rather an art than a science. Therefore alternative methods are very important and fortunately are under consideration.

Patrick Janot's approach certainly is an important alternative method directly accessing $\alpha(M_Z^2)$ with very different systematics. A challenging project.

Another interesting option is an improved radiative return measurement of $\sigma(e^+e^- \to$ hadrons) at the GigaZ, allowing for directly improving dispersion integral input, which would include all resonances and thresholds in one experiment!

In any case, on paper, $e^-\mu^+ \to e^-\mu^+$ looks to be the ideal process to perform an unambiguous measurement of $\alpha(-Q^2)$, which determines the LO HVP to a_μ as well as the non-perturbative part of $\alpha(s)$!

Lattice QCD results are very close to becoming competitive here as well. Thus, in the end, we will have alternatives available allowing for important improvements and crosschecks.

The improvement obtained by reducing the experimental error to 1% in the range from ϕ to 3 GeV would allow one to choose a higher cut point e.g. for $\sqrt{M_0} = 3.0$ GeV. One then can balance the importance of data vs. pQCD differently. This would provide further important consolidation of results. For a 3 GeV cut one gets $\Delta\alpha_{\text{had}}(-M_0^2) = 82.21 \pm 0.88[0.38]$ in 10^{-4}. The QCD contribution is then smaller as well as safer because the mass effects that are responsible for the larger uncertainty of the pQCD prediction also gets substantially reduced. In view that a massive 4-loop QCD calculation is a challenge, the possibility to optimize the choice of split scale M_0 would be very useful. Therefore the ILC/FCC-ee community should actively support these activities as an integral part of e^+e^--collider precision physics program!

8 Addendum: the coupling α_2, M_W and $\sin^2\Theta_f$

Besides α also the $SU(2)$ gauge coupling $\alpha_2 = g^2/(4\pi)$ is running and thereby affected by non-perturbative hadronic effects [77, 89, 90]. Related with the $U_Y(1) \otimes SU_L(2)$ gauge couplings, is the running oft the weak mixing parameter $\sin^2\Theta_f$, which is actually defined by the ratio α/α_2. In [77, 89, 90] the hadronic effects have been evaluated by means of DRs in terms of e^+e^- data with appropriate flavor separation and reweighting. Commonly, a much simpler approach is adopted in studies of the running of $\sin^2\Theta_f$, namely by using pQCD with effective quark masses [91–94], which have been determined elsewhere.

Given $g \equiv g_2$ and the Higgs VEV v then $M_W^2 = \frac{g^2 v^2}{4} = \frac{\pi \alpha_2}{\sqrt{2} G_\mu}$. The running $\sin^2\Theta_f(s)$ relates electromagnetic to weak neutral channel mixing at the LEP scale to low energy $\nu_e e$ scattering as

$$\sin^2\Theta_{\text{lep}}(M_Z^2) = \left\{ \frac{1 - \Delta\alpha_2}{1 - \Delta\alpha} + \Delta_{\nu_\mu e, \text{vertex+box}} + \Delta\kappa_{e, \text{vertex}} \right\} \sin^2\Theta_{\nu_\mu e}(0) . \tag{23}$$

The first correction from the running coupling ratio is largely compensated by the ν_μ charge-radius, which dominates the second term. The ratio $\sin^2\Theta_{\nu_\mu e}/\sin^2\Theta_{\text{lep}}$ is close to 1.002, independent of top and Higgs mass. Note that errors in the ratio $\frac{1-\Delta\alpha_2}{1-\Delta\alpha}$ can be taken to be 100% correlated and thus largely cancel. A similar relation between $\sin^2\Theta_{\text{lep}}(M_Z^2)$ and the weak mixing angle appearing in polarized Møller scattering asymmetries has been worked out in [91, 92]. It includes specific bosonic contribution $\Delta\kappa_b(Q^2)$ such that

$$\kappa(s = -Q^2) = \frac{1 - \Delta\alpha_2(s)}{1 - \Delta\alpha(s)} + \Delta\kappa_b(Q^2) - \Delta\kappa_b(0) \tag{24}$$

where , in our low energy scheme, we require $\kappa(Q^2) = 1$ at $Q^2 = 0$. Explicitly [91, 92], at 1-loop order

$$\Delta\kappa_b(Q^2) = -\frac{\alpha}{2\pi s_W}\left\{ -\frac{42 c_W + 1}{12} \ln c_W + \frac{1}{18} - \left(\frac{r}{2}\ln\xi - 1\right)\left[(7 - 4z)c_W \right.\right. \tag{25}$$

$$\left.\left. + \frac{1}{6}(1 + 4z)\right] - z\left[\frac{3}{4} - z + \left(z - \frac{2}{3}\right) r \ln\xi + z(2 - z) \ln^2\xi\right]\right\} ,$$

$$\Delta\kappa_b(0) = -\frac{\alpha}{2\pi s_W}\left\{ -\frac{42 c_W + 1}{12}\ln c_W + \frac{1}{18} + \frac{6 c_W + 7}{18}\right\}, \tag{26}$$

with $z = M_W^2/Q^2$, $r = \sqrt{1 + 4z}$, $\xi = \frac{r+1}{r-1}$, $s_W = \sin^2\Theta_W$ and $c_W = \cos^2\Theta_W$. Results obtained in [91, 92] based on one-loop perturbation theory using light quark masses $m_u = m_d = m_s = 100$ MeV are compared with results obtained in our non-perturbative approach in Fig. 17.

How to evaluate the leading non-perturbative hadronic corrections to α_2? Like in the case of α they are related to quark-loop contributions to gauge-boson self-energies (SE) $\gamma\gamma$, γZ, ZZ and WW, in particular those involving the photon, which exhibit large leading logarithms. In order to disentangle the leading corrections decompose the self-energy functions as follows ($s_\Theta^2 = e^2/g^2$; $c_\Theta^2 = 1 - s_\Theta^2$)

$$
\begin{aligned}
\Pi^{\gamma\gamma} &= e^2 \ \hat{\Pi}^{\gamma\gamma}, \\
\Pi^{Z\gamma} &= \frac{eg}{c_\Theta} \ \hat{\Pi}_V^{3\gamma} \quad - \quad \frac{e^2 s_\Theta}{c_\Theta} \ \hat{\Pi}_V^{\gamma\gamma}, \\
\Pi^{ZZ} &= \frac{g^2}{c_\Theta^2} \ \hat{\Pi}_{V-A}^{33} \quad - \quad 2 \frac{e^2}{c_\Theta^2} \ \hat{\Pi}_V^{3\gamma} \quad + \quad \frac{e^2 s_\Theta^2}{c_\Theta^2} \ \hat{\Pi}_V^{\gamma\gamma}, \\
\Pi^{WW} &= g^2 \ \hat{\Pi}_{V-A}^{+-},
\end{aligned}
\tag{27}
$$

with $\hat{\Pi}(s) = \hat{\Pi}(0) + s \Pi'(s)$, we find the leading hadronic corrections

$$
\Delta\alpha_{\mathrm{had}}^{(5)}(s) = -e^2 \left[\mathrm{Re}\Pi'^{\gamma\gamma}(s) - \Pi'^{\gamma\gamma}(0) \right], \tag{28}
$$

$$
\Delta\alpha_{2\,\mathrm{had}}^{(5)}(s) = -\frac{e^2}{s_\Theta^2} \left[\mathrm{Re}\Pi'^{3\gamma}(s) - \Pi'^{3\gamma}(0) \right], \tag{29}
$$

which exhibit the leading hadronic non-perturbative parts, i.e. the ones involving the photon field via mixing. Besides $\Delta\alpha_{\mathrm{had}}^{(5)}(s)$ also $\Delta\alpha_{2\,\mathrm{had}}^{(5)}(s)$ can then be obtained in terms of e^+e^--data together with isospin flavor separation of (u, d) and s components

$$
\Pi_{ud}^{3\gamma} = \frac{1}{2} \Pi_{ud}^{\gamma\gamma} \; ; \quad \Pi_s^{3\gamma} = \frac{3}{4} \Pi_s^{\gamma\gamma} \tag{30}
$$

and for resonance contributions

$$
\begin{aligned}
\Pi^{\gamma\gamma} &= \Pi^{(\rho)} + \Pi^{(\omega)} + \Pi^{(\phi)} + \cdots \\
\Pi^{3\gamma} &= \frac{1}{2} \Pi^{(\rho)} + \frac{3}{4} \Pi^{(\phi)} + \cdots
\end{aligned}
\tag{31}
$$

We remind that gauge-boson SE are potentially very sensitive to new physics (oblique corrections) and the discovery of what is missing in the SM may be obscured by non-perturbative hadronic effects. Therefore it is important to reduce the related uncertainties. Interestingly, flavor separation assuming OZI violating terms to be small implies a perturbative reweighting, which however has been shown to disagrees with lattice QCD results [95–98]! Indeed, the "wrong" perturbative flavor weighting

$$
\Pi_{ud}^{3\gamma} = \frac{9}{20} \Pi_{ud}^{\gamma\gamma} \; ; \quad \Pi_s^{3\gamma} = \frac{3}{4} \Pi_s^{\gamma\gamma}
$$

clearly mismatch lattice results, while the replacement $\frac{9}{20} \Rightarrow \frac{10}{20}$ is in good agreement. This also means the OZI suppressed contributions should be at the 5% level and not negligibly small. Actually, if we assume flavor $SU(3)$ symmetry to be an acceptable approximation one obtains

$$
\Pi_{uds}^{3\gamma} = \frac{1}{2} \Pi_{uds}^{\gamma\gamma},
$$

which does not require any flavor separation in the uds-sector, i.e. up to the charm threshold at about 3.1 GeV. The Fig. 15 shows a lattice QCD test of two flavor separation schemes. One labeled "$SU(2)$" denotes the perturbative reweighting advocated in [91–94] and the other one labeled "$SU(3)$" represents the one proposed in [89]. Lattice data clearly disprove pQCD reweighting for the uds-sector!
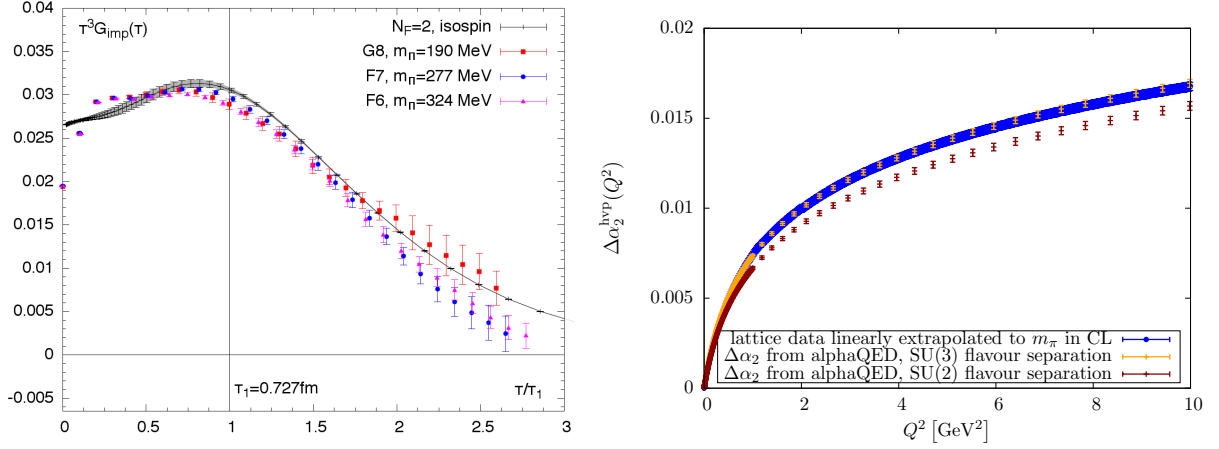
Fig. 15: Testing flavor separation in lattice QCD. Left: a rough test by checking the Euclidean time correlators clearly favors the flavor separation of (31) [95–97], while the pQCD reweighting (not displayed) badly fails. Right: the renormalized photon self-energy at Euclidean Q^2 [98] is in good agreement with the flavor $SU(3)$ limit, while again it fails with the $SU(2)$ case which coincides with perturbative reweighting.
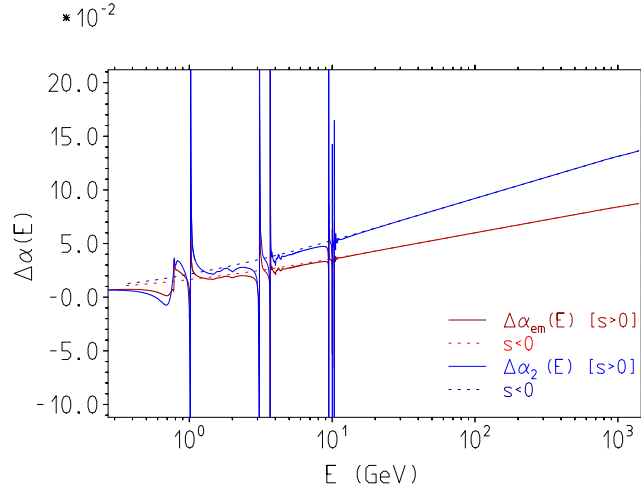

Fig. 16: $\Delta\alpha_{\mathrm{QED}}(E)$ and $\Delta\alpha_2(E)$ as functions of energy E in the time-like and space-like domain. The smooth space-like correction (dashed line) agrees rather well with the non-resonant "background" above the ϕ-resonance (kind of duality). In resonance regions as expected "agreement" is observed in the mean, with huge local deviations.

This also shows that pQCD-type predictions based on effective quark masses cannot be accurate. This criticism also applies in cases where the effective quark masses have been obtained by fitting $\Delta\alpha_{\mathrm{had}}^{(5)}(s)$. Even more so when constituent quark masses are used.

The updated $\sin^2\Theta_W(s)$ is shown in Fig. 17 for time-like as well as for space-like momentum transfer. Note that $\sin^2\Theta_W(0)/\sin^2\Theta_W(M_Z^2) = 1.02876$ a 3% correction is established at 6.5 σ. Except for the LEP and SLD points (which deviate by 1.8 σ), all existing measurements are of rather limited accuracy, unfortunately. Upcoming experiments will improve results at low space-like Q substantially. We remind that $\sin^2\Theta_{\ell\,\mathrm{eff}}$ exhibiting a specific dependence on the gauge boson self-energies is an excellent monitor for New Physics. At pre-LHC times it has been the predestinated monitor for
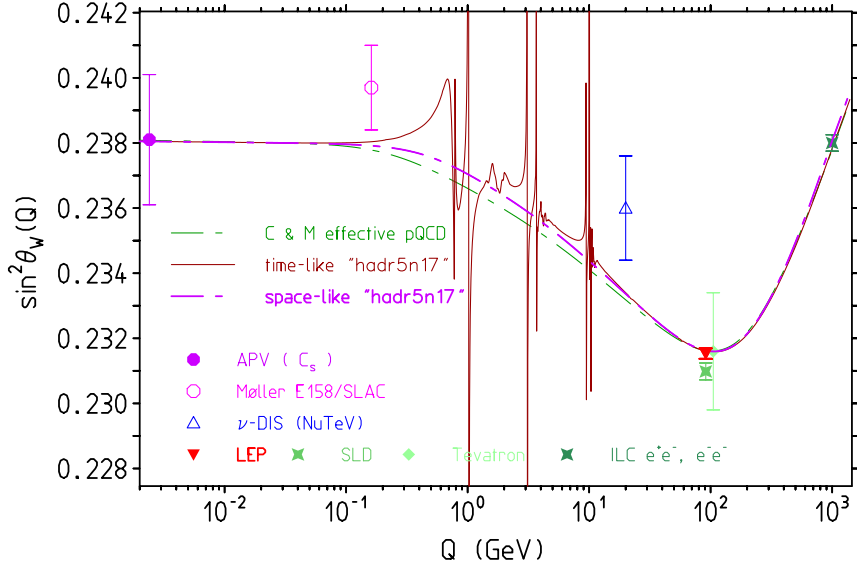
Fig. 17: $\sin^2 \Theta_W(Q)$ as a function of Q in the time-like and space-like region. Hadronic uncertainties are included but barely visible in this plot. Uncertainties from the input parameter $\sin^2 \Theta_W(0) = 0.23822(100)$ or $\sin^2 \Theta_W(M_Z^2) = 0.23153(16)$ are not shown. Note the substantial difference from applying pQCD with effective quark masses. Future FCC-ee/ILC measurements at 1 TeV would be sensitive to Z', H^{--} etc.

virtual Higgs particle effects and a corresponding limiter for the Higgs boson mass.

Acknowledgments

References

[1] T. Hambye, K. Riesselmann, Matching conditions and Higgs mass upper bounds revisited, Phys. Rev. D55 (1997) 7255–7262. arXiv:hep-ph/9610272, doi:10.1103/PhysRevD.55.7255.

[2] F. Jegerlehner, M. Yu. Kalmykov, B. A. Kniehl, On the difference between the pole and the $\overline{MS}$ masses of the top quark at the electroweak scale, Phys. Lett. B722 (2013) 123–129. arXiv:1212.4319, doi:10.1016/j.physletb.2013.04.012.

[3] F. Jegerlehner, The Standard model as a low-energy effective theory: what is triggering the Higgs mechanism?, Acta Phys. Polon. B45 (6) (2014) 1167. arXiv:1304.7813, doi:10.5506/APhysPolB.45.1167.

[4] F. Jegerlehner, Higgs inflation and the cosmological constant, Acta Phys. Polon. B45 (6) (2014) 1215. arXiv:1402.3738, doi:10.5506/APhysPolB.45.1215.

[5] F. Jegerlehner, M. Yu. Kalmykov, B. A. Kniehl, Self-consistence of the Standard Model via the renormalization group analysis, J. Phys. Conf. Ser. 608 (1) (2015) 012074. arXiv:1412.4215, doi:10.1088/1742-6596/608/1/012074.

[6] F. Bezrukov, M. Yu. Kalmykov, B. A. Kniehl, M. Shaposhnikov, Higgs Boson Mass and New Physics, JHEP 10 (2012) 140, [,275(2012)]. arXiv:1205.2893, doi:10.1007/JHEP10(2012)140.

[7] G. Degrassi, S. Di Vita, J. Elias-Miro, J. R. Espinosa, G. F. Giudice, G. Isidori, A. Strumia, Higgs mass and vacuum stability in the Standard Model at NNLO, JHEP 08 (2012) 098. arXiv:1205.6497, doi:10.1007/JHEP08(2012)098.

[8] J. S. Huxley, T. H. Huxley, Evolution and Ethics:, 1893-1943, The Pilot Press, London, 1947.

[9] R. R. Akhmetshin, et al., Reanalysis of hadronic cross-section measurements at CMD-2, Phys. Lett. B578 (2004) 285–289. arXiv:hep-ex/0308008, doi:10.1016/j.physletb.2003.10.108.

[10] V. M. Aul'chenko, et al., Measurement of the pion form-factor in the range 1.04 GeV to 1.38 GeV with the CMD-2 detector, JETP Lett. 82 (2005) 743–747, [Pisma Zh. Eksp. Teor. Fiz.82,841(2005)]. arXiv:hep-ex/0603021, doi:10.1134/1.2175241.

[11] V. M. Aul'chenko, et al., Measurement of the $e^+e^- \to \pi^+\pi^-$ cross section with the CMD-2 detector in the 370 - 520-MeV c.m. energy range, JETP Lett. 84 (2006) 413–417, [Pisma Zh. Eksp. Teor. Fiz.84,491(2006)]. arXiv:hep-ex/0610016, doi:10.1134/S0021364006200021.

[12] R. R. Akhmetshin, et al., High-statistics measurement of the pion form factor in the rho-meson energy range with the CMD-2 detector, Phys. Lett. B648 (2007) 28–38. arXiv:hep-ex/0610021, doi:10.1016/j.physletb.2007.01.073.

[13] M. N. Achasov, et al., Update of the $e^+e^- \to \pi^+\pi^-$ cross-section measured by SND detector in the energy region 400 MeV $< s^{1/2} <$ 1000 MeV, J. Exp. Theor. Phys. 103 (2006) 380–384, [Zh. Eksp. Teor. Fiz.130,437(2006)]. arXiv:hep-ex/0605013, doi:10.1134/S106377610609007X.

[14] A. Aloisio, et al., Measurement of $\sigma(e^+e^- \to \pi^+\pi^-\gamma)$ and extraction of $\sigma(e^+e^- \to \pi^+\pi^-)$ below 1 GeV with the KLOE detector, Phys. Lett. B606 (2005) 12–24. arXiv:hep-ex/0407048, doi:10.1016/j.physletb.2004.11.068.

[15] F. Ambrosino, et al., Measurement of $\sigma(e^+e^- \to \pi^+\pi^-\gamma(\gamma))$ and the dipion contribution to the muon anomaly with the KLOE detector, Phys. Lett. B670 (2009) 285–291. arXiv:0809.3950, doi:10.1016/j.physletb.2008.10.060.

[16] F. Ambrosino, et al., Measurement of $\sigma(e^+e^- \to \pi^+\pi^-)$ from threshold to 0.85 GeV^2 using Initial State Radiation with the KLOE detector, Phys. Lett. B700 (2011) 102–110. arXiv:1006.5313, doi:10.1016/j.physletb.2011.04.055.

[17] D. Babusci, et al., Precision measurement of $\sigma(e^+e^- \to \pi^+\pi^-\gamma)/\sigma(e^+e^- \to \mu^+\mu^-\gamma)$ and determination of the $\pi^+\pi^-$ contribution to the muon anomaly with the KLOE detector, Phys. Lett. B720 (2013) 336–343. arXiv:1212.4524, doi:10.1016/j.physletb.2013.02.029.

[18] A. Anastasi, et al., Combination of KLOE $\sigma(e^+e^- \to \pi^+\pi^-\gamma(\gamma))$ measurements and determination of $a_\mu^{\pi^+\pi^-}$ in the energy range $0.10 < s < 0.95$ GeV^2, JHEP 03 (2018) 173. arXiv:1711.03085, doi:10.1007/JHEP03(2018)173.

[19] G. Venanzoni, From Hadronic Cross Section to the measurement of the Vacuum Polarization at KLOE: a fascinating endeavour, EPJ Web Conf. 166 (2018) 00021. arXiv:1705.10365, doi:10.1051/epjconf/201816600021.

[20] B. Aubert, et al., Precise measurement of the $e^+e^- \to \pi^+\pi^-(\gamma)$ cross section with the Initial State Radiation method at BABAR, Phys. Rev. Lett. 103 (2009) 231801. arXiv:0908.3589, doi:10.1103/PhysRevLett.103.231801.

[21] J. P. Lees, et al., Precise Measurement of the $e^+e^- \to \pi^+\pi^-(\gamma)$ Cross Section with the Initial-

State Radiation Method at BABAR, Phys. Rev. D86 (2012) 032013. `arXiv:1205.2228`, `doi: 10.1103/PhysRevD.86.032013`.

[22] M. Ablikim, et al., Measurement of the $e^+e^- \to \pi^+\pi^-$ cross section between 600 and 900 MeV using initial state radiation, Phys. Lett. B753 (2016) 629–638. `arXiv:1507.08188`, `doi:10.1016/j.physletb.2015.11.043`.

[23] T. Xiao, S. Dobbs, A. Tomaradze, K. K. Seth, G. Bonvicini, Precision Measurement of the Hadronic Contribution to the Muon Anomalous Magnetic Moment, Phys. Rev. D97 (3) (2018) 032012. `arXiv:1712.04530`, `doi:10.1103/PhysRevD.97.032012`.

[24] B. Aubert, et al., Study of $e^+e^- \to \pi^+\pi^-\pi^0$ process using initial state radiation with BaBar, Phys. Rev. D70 (2004) 072004. `arXiv:hep-ex/0408078`, `doi:10.1103/PhysRevD.70.072004`.

[25] B. Aubert, et al., The $e^+e^- \to \pi^+\pi^-\pi^+\pi^-$, $K^+K^-\pi^+\pi^-$, and $K^+K^-K^+K^-$ cross sections at center-of-mass energies 0.5 GeV - 4.5 GeV measured with initial-state radiation, Phys. Rev. D71 (2005) 052001. `arXiv:hep-ex/0502025`, `doi:10.1103/PhysRevD.71.052001`.

[26] B. Aubert, et al., A Study of $e^+e^- \to p\bar{p}$ using initial state radiation with BABAR, Phys. Rev. D73 (2006) 012005. `arXiv:hep-ex/0512023`, `doi:10.1103/PhysRevD.73.012005`.

[27] B. Aubert, et al., The $e^+e^- \to 3(\pi^+\pi^-), 2(\pi^+\pi^-\pi^0)$ and $K^+K^-2(\pi^+\pi^-)$ cross sections at center-of-mass energies from production threshold to 4.5 GeV measured with initial-state radiation, Phys. Rev. D73 (2006) 052003. `arXiv:hep-ex/0602006`, `doi:10.1103/PhysRevD.73.052003`.

[28] B. Aubert, et al., The $e^+e^- \to 2(\pi^+\pi^-)\pi^0$, $2(\pi^+\pi^-)\eta$, $K^+K^-\pi^+\pi^-\pi^0$ and $K^+K^-\pi^+\pi^-\eta$ Cross Sections Measured with Initial-State Radiation, Phys. Rev. D76 (2007) 092005, [Erratum: Phys. Rev.D77,119902(2008)]. `arXiv:0708.2461`, `doi:10.1103/PhysRevD.77.119902, 10.1103/PhysRevD.76.092005`.

[29] B. Aubert, et al., Measurements of $e^+e^- \to K^+K^-\eta$, $K^+K^-\pi^0$ and $K^0_s K^{\pm}\pi^{\mp}$ cross- sections using initial state radiation events, Phys. Rev. D77 (2008) 092002. `arXiv:0710.4451`, `doi:10.1103/PhysRevD.77.092002`.

[30] J. P. Lees, et al., Initial-State Radiation Measurement of the $e^+e^- \to \pi^+\pi^-\pi^+\pi^-$ Cross Section, Phys. Rev. D85 (2012) 112009. `arXiv:1201.5677`, `doi:10.1103/PhysRevD.85.112009`.

[31] J. P. Lees, et al., Cross Sections for the Reactions $e^+e^- \to K^+K^-\pi^+\pi^-$, $K^+K^-\pi^0\pi^0$, and $K^+K^-K^+K^-$ Measured Using Initial-State Radiation Events, Phys. Rev. D86 (2012) 012008. `arXiv:1103.3001`, `doi:10.1103/PhysRevD.86.012008`.

[32] J. P. Lees, et al., Study of $e^+e^- \to p\bar{p}$ via initial-state radiation at BABAR, Phys. Rev. D87 (9) (2013) 092005. `arXiv:1302.0055`, `doi:10.1103/PhysRevD.87.092005`.

[33] J. P. Lees, et al., Precision measurement of the $e^+e^- \to K^+K^-(\gamma)$ cross section with the initial-state radiation method at BABAR, Phys. Rev. D88 (3) (2013) 032013. `arXiv:1306.3600`, `doi:10.1103/PhysRevD.88.032013`.

[34] J. P. Lees, et al., Cross sections for the reactions $e^+e^- \to K^0_S K^0_L$, $K^0_S K^0_L \pi^+\pi^-$, $K^0_S K^0_S \pi^+\pi^-$, and $K^0_S K^0_S K^+K^-$ from events with initial-state radiation, Phys. Rev. D89 (9) (2014) 092002. `arXiv:1403.7593`, `doi:10.1103/PhysRevD.89.092002`.

[35] J. P. Lees, et al., Study of the reactions $e^+e^- \to \pi^+\pi^-\pi^0\pi^0\pi^0\gamma$ and $\pi^+\pi^-\pi^0\pi^0\eta\gamma$ at center-of-mass energies from threshold to 4.35 GeV using initial-state radiation, Phys. Rev. D98 (11) (2018) 112015. `arXiv:1810.11962`, `doi:10.1103/PhysRevD.98.112015`.

[36] M. Davier, e^+e^- results from BABAR and their impact on the muon $g-2$ prediction, Nucl. Part. Phys. Proc. 260 (2015) 102–106. `doi:10.1016/j.nuclphysbps.2015.02.021`.

[37] M. Davier, A. Hoecker, B. Malaescu, Z. Zhang, Hadron Contribution to Vacuum Polarisation, Adv. Ser. Direct. High Energy Phys. 26 (2016) 129–144. `doi:10.1142/9789814733519_`

0007.

[38] R. R. Akhmetshin, et al., Study of the process $e^+e^- \to 3(\pi^+\pi^-)$ in the c.m.energy range 1.5–2.0 gev with the cmd-3 detector, Phys. Lett. B723 (2013) 82–89. arXiv:1302.0053, doi:10.1016/j.physletb.2013.04.065.

[39] R. R. Akhmetshin, et al., Study of the process $e^+e^- \to p\bar{p}$ in the c.m. energy range from threshold to 2 GeV with the CMD-3 detector, Phys. Lett. B759 (2016) 634–640. arXiv:1507.08013, doi:10.1016/j.physletb.2016.04.048.

[40] E. A. Kozyrev, et al., Study of the process $e^+e^- \to K_S^0 K_L^0$ in the center-of-mass energy range 1004–1060 MeV with the CMD-3 detector at the VEPP-2000 e^+e^- collider, Phys. Lett. B760 (2016) 314–319. arXiv:1604.02981, doi:10.1016/j.physletb.2016.07.003.

[41] M. N. Achasov, et al., Study of the process $e^+e^- \to n\bar{n}$ at the VEPP-2000 e^+e^- collider with the SND detector, Phys. Rev. D90 (11) (2014) 112007. arXiv:1410.3188, doi:10.1103/PhysRevD.90.112007.

[42] V. M. Aulchenko, et al., Measurement of the $e^+e^- \to \eta\pi^+\pi^-$ cross section in the center-of-mass energy range 1.22-2.00 GeV with the SND detector at the VEPP-2000 collider, Phys. Rev. D91 (5) (2015) 052013. arXiv:1412.1971, doi:10.1103/PhysRevD.91.052013.

[43] M. N. Achasov, et al., Study of the reaction $e^+e^- \to \pi^0\gamma$ with the SND detector at the VEPP-2M collider, Phys. Rev. D93 (9) (2016) 092001. arXiv:1601.08061, doi:10.1103/PhysRevD.93.092001.

[44] M. N. Achasov, et al., Study of the process $e^+e^- \to \omega\eta\pi^0$ in the energy range $\sqrt{s} < 2$ GeV with the SND detector, Phys. Rev. D94 (3) (2016) 032010. arXiv:1606.06481, doi:10.1103/PhysRevD.94.032010.

[45] M. N. Achasov, et al., Measurement of the $e^+e^- \to \omega\eta$ cross section below $\sqrt{s} = 2$ GeV, Phys. Rev. D94 (9) (2016) 092002. arXiv:1607.00371, doi:10.1103/PhysRevD.94.092002.

[46] M. N. Achasov, et al., Measurement of the $e^+e^- \to K^+K^-$ cross section in the energy range $\sqrt{s} = 1.05 - 2.0$ GeV, Phys. Rev. D94 (11) (2016) 112006. arXiv:1608.08757, doi:10.1103/PhysRevD.94.112006.

[47] M. N. Achasov, et al., Updated measurement of the $e^+e^- \to \omega\pi^0 \to \pi^0\pi^0\gamma$ cross section with the SND detector, Phys. Rev. D94 (11) (2016) 112001. arXiv:1610.00235, doi:10.1103/PhysRevD.94.112001.

[48] J. Z. Bai, et al., Measurement of the total cross-section for hadronic production by e^+e^- annihilation at energies between 2.6 GeV - 5 GeV, Phys. Rev. Lett. 84 (2000) 594–597. arXiv:hep-ex/9908046, doi:10.1103/PhysRevLett.84.594.

[49] J. Z. Bai, et al., Measurements of the cross-section for $e^+e^- \to$ hadrons at center-of-mass energies from 2 GeV to 5 GeV, Phys. Rev. Lett. 88 (2002) 101802. arXiv:hep-ex/0102003, doi:10.1103/PhysRevLett.88.101802.

[50] M. Ablikim, et al., R value measurements for e^+e^- annihilation at 2.60 GeV, 3.07 GeV and 3.65 GeV, Phys. Lett. B677 (2009) 239–245. arXiv:0903.0900, doi:10.1016/j.physletb.2009.05.055.

[51] V. V. Anashin, et al., Measurement of R_{uds} and R between 3.12 and 3.72 GeV at the KEDR detector, Phys. Lett. B753 (2016) 533–541. arXiv:1510.02667, doi:10.1016/j.physletb.2015.12.059.

[52] V. V. Anashin, et al., Measurement of R between 1.84 and 3.05 GeV at the KEDR detector, Phys. Lett. B770 (2017) 174–181. arXiv:1610.02827, doi:10.1016/j.physletb.2017.04.073.

[53] R. V. Harlander, M. Steinhauser, rhad: A Program for the evaluation of the hadronic R ratio in the perturbative regime of QCD, Comput. Phys. Commun. 153 (2003) 244–274. `arXiv:hep-ph/0212294`, `doi:10.1016/S0010-4655(03)00204-2`.

[54] S. Eidelman, F. Jegerlehner, Hadronic contributions to $g - 2$ of the leptons and to the effective fine structure constant $\alpha(M_Z^2)$, Z. Phys. C67 (1995) 585–602. `arXiv:hep-ph/9502298`, `doi:10.1007/BF01553984`.

[55] M. Davier, A. Hoecker, B. Malaescu, Z. Zhang, Reevaluation of the hadronic vacuum polarisation contributions to the Standard Model predictions of the muon $g - 2$ and $\alpha(m_Z^2)$ using newest hadronic cross-section data, Eur. Phys. J. C77 (12) (2017) 827. `arXiv:1706.09436`, `doi:10.1140/epjc/s10052-017-5161-6`.

[56] A. Maier, P. Marquard, Validity of Padé approximations in vacuum polarization at three- and four-loop order, Phys. Rev. D97 (5) (2018) 056016. `arXiv:1710.03724`, `doi:10.1103/PhysRevD.97.056016`.

[57] F. Jegerlehner, Leading-order hadronic contribution to the electron and muon $g - 2$, EPJ Web Conf. 118 (2016) 01016. `arXiv:1511.04473`, `doi:10.1051/epjconf/201611801016`.

[58] A. Anastasi, et al., Measurement of the running of the fine structure constant below 1 GeV with the KLOE Detector, Phys. Lett. B767 (2017) 485–492. `arXiv:1609.06631`, `doi:10.1016/j.physletb.2016.12.016`.

[59] S. L. Adler, Some Simple Vacuum Polarization Phenomenology: $e^+e^- \rightarrow$ Hadrons: The μ -Mesic Atom x-Ray Discrepancy and $g_\mu - 2$, Phys. Rev. D10 (1974) 3714, [,445(1974)]. `doi:10.1103/PhysRevD.10.3714`.

[60] S. Eidelman, F. Jegerlehner, A. L. Kataev, O. Veretin, Testing nonperturbative strong interaction effects via the Adler function, Phys. Lett. B454 (1999) 369–380. `arXiv:hep-ph/9812521`, `doi:10.1016/S0370-2693(99)00389-5`.

[61] F. Jegerlehner, Hadronic effects in $(g - 2)_\mu$ and $\alpha_{QED}(M_Z^2)$: Status and perspectives, in: Radiative corrections: Application of quantum field theory to phenomenology. Proceedings, 4th International Symposium, RADCOR'98, Barcelona, Spain, September 8-12, 1998, 1999, pp. 75–89. `arXiv:hep-ph/9901386`.

[62] F. Jegerlehner, Hadronic vacuum polarization effects in $\alpha_{em}(M_Z^2)$, in: Electroweak precision data and the Higgs mass. Proceedings, Workshop, Zeuthen, Germany, February 28-March 1, 2003, 2003, pp. 97–112. `arXiv:hep-ph/0308117`.

[63] F. Jegerlehner, The Running fine structure constant $\alpha(E)$ via the Adler function, Nucl. Phys. Proc. Suppl. 181-182 (2008) 135–140. `arXiv:0807.4206`, `doi:10.1016/j.nuclphysbps.2008.09.010`.

[64] M. Benayoun, P. David, L. DelBuono, F. Jegerlehner, Muon $g - 2$ estimates: can one trust effective Lagrangians and global fits?, Eur. Phys. J. C75 (12) (2015) 613. `arXiv:1507.02943`, `doi:10.1140/epjc/s10052-015-3830-x`.

[65] M. Benayoun, L. DelBuono, F. Jegerlehner, BHLS$_2$, a New Breaking of the HLS Model and its Phenomenology`arXiv:1903.11034`.

[66] F. Jegerlehner, O. V. Tarasov, Exact mass dependent two loop $\bar{\alpha}(s)(Q^2)$ in the background MOM renormalization scheme, Nucl. Phys. B549 (1999) 481–498. `arXiv:hep-ph/9809485`, `doi:10.1016/S0550-3213(99)00141-8`.

[67] K. G. Chetyrkin, J. H. Kühn, M. Steinhauser, Three loop polarization function and $O(\alpha_s^2)$ corrections to the production of heavy quarks, Nucl. Phys. B482 (1996) 213–240. `arXiv:hep-ph/9606230`, `doi:10.1016/S0550-3213(96)00534-2`.

[68] K. G. Chetyrkin, R. Harlander, J. H. Kühn, M. Steinhauser, Mass corrections to the vector current correlator, Nucl. Phys. B503 (1997) 339–353. `arXiv:hep-ph/9704222`, `doi:10.1016/S0550-3213(97)00383-0`.

[69] K. G. Chetyrkin, J. H. Kühn, M. Steinhauser, Heavy quark current correlators to $O(\alpha_s^2)$, Nucl. Phys. B505 (1997) 40–64. `arXiv:hep-ph/9705254`, `doi:10.1016/S0550-3213(97)00481-1`.

[70] M. A. Shifman, A. I. Vainshtein, V. I. Zakharov, QCD and Resonance Physics. Theoretical Foundations, Nucl. Phys. B147 (1979) 385–447. `doi:10.1016/0550-3213(79)90022-1`.

[71] M. A. Shifman, A. I. Vainshtein, V. I. Zakharov, QCD and Resonance Physics: Applications, Nucl. Phys. B147 (1979) 448–518. `doi:10.1016/0550-3213(79)90023-3`.

[72] D. V. Shirkov, I. L. Solovtsov, Analytic model for the QCD running coupling with universal $\alpha_s(0)$ value, Phys. Rev. Lett. 79 (1997) 1209–1212. `arXiv:hep-ph/9704333`, `doi:10.1103/PhysRevLett.79.1209`.

[73] M. Bruno, M. Dalla Brida, P. Fritzsch, T. Korzec, A. Ramos, S. Schaefer, H. Simma, S. Sint, R. Sommer, QCD Coupling from a Nonperturbative Determination of the Three-Flavor Λ Parameter, Phys. Rev. Lett. 119 (10) (2017) 102001. `arXiv:1706.03821`, `doi:10.1103/PhysRevLett.119.102001`.

[74] M. Steinhauser, Leptonic contribution to the effective electromagnetic coupling constant up to three loops, Phys. Lett. B429 (1998) 158–161. `arXiv:hep-ph/9803313`, `doi:10.1016/S0370-2693(98)00503-6`.

[75] G. Abbiendi, et al., Measuring the leading hadronic contribution to the muon g-2 via μe scattering, Eur. Phys. J. C77 (3) (2017) 139. `arXiv:1609.08987`, `doi:10.1140/epjc/s10052-017-4633-z`.

[76] A. Keshavarzi, D. Nomura, T. Teubner, Muon $g-2$ and $\alpha(M_Z^2)$: a new data-based analysis, Phys. Rev. D97 (11) (2018) 114025. `arXiv:1802.02995`, `doi:10.1103/PhysRevD.97.114025`.

[77] F. Jegerlehner, Variations on Photon Vacuum Polarization`arXiv:1711.06089`.

[78] P. Janot, Direct measurement of $\alpha_{QED}(m_Z^2)$ at the FCC-ee, JHEP 02 (2016) 053, [Erratum: JHEP11,164(2017)]. `arXiv:1512.05544`, `doi:10.1007/JHEP02(2016)053,10.1007/JHEP11(2017)164`.

[79] A. Blondel, et al., Standard Model Theory for the FCC-ee: The Tera-Z, in: Mini Workshop on Precision EW and QCD Calculations for the FCC Studies : Methods and Techniques CERN, Geneva, Switzerland, January 12-13, 2018, 2018, p. 243pp. `arXiv:1809.01830`.

[80] I. Dubovyk, A. Freitas, J. Gluza, T. Riemann, J. Usovitsch, Complete electroweak two-loop corrections to Z boson production and decay, Phys. Lett. B783 (2018) 86–94. `arXiv:1804.10236`, `doi:10.1016/j.physletb.2018.06.037`.

[81] P. Azzurri, et al., Physics Behind Precision`arXiv:1703.01626`.

[82] S. Jadach, W. Płaczek, M. Skrzypek, B. F. L. Ward, S. A. Yost, The path to 0.01% theoretical luminosity precision for the FCC-ee, Phys. Lett. B790 (2019) 314–321. `arXiv:1812.01004`, `doi:10.1016/j.physletb.2019.01.012`.

[83] S. Jadach, et al., Event generators for Bhabha scattering, in: CERN Workshop on LEP2 Physics (followed by 2nd meeting, 15-16 Jun 1995 and 3rd meeting 2-3 Nov 1995) Geneva, Switzerland, February 2-3, 1995, 1996, pp. 229–298. `arXiv:hep-ph/9602393`.

[84] A. Arbuzov, et al., The Present theoretical error on the Bhabha scattering cross-section in the luminometry region at LEP, Phys. Lett. B383 (1996) 238–242. `arXiv:hep-ph/9605239`, `doi:10.1016/0370-2693(96)00733-2`.

[85] P. Mastrolia, M. Passera, A. Primo, U. Schubert, Master integrals for the NNLO virtual corrections to μe scattering in QED: the planar graphs, JHEP 11 (2017) 198. `arXiv:1709.07435`, `doi:10.1007/JHEP11(2017)198`.

[86] S. Di Vita, S. Laporta, P. Mastrolia, A. Primo, U. Schubert, Master integrals for the NNLO virtual corrections to μe scattering in QED: the non-planar graphs, JHEP 09 (2018) 016. `arXiv:1806.08241`, `doi:10.1007/JHEP09(2018)016`.

[87] M. Fael, Hadronic corrections to μ-e scattering at NNLO with space-like data, JHEP 02 (2019) 027. `arXiv:1808.08233`, `doi:10.1007/JHEP02(2019)027`.

[88] M. Alacevich, C. M. Carloni Calame, M. Chiesa, G. Montagna, O. Nicrosini, F. Piccinini, Muon-electron scattering at NLO, JHEP 02 (2019) 155. `arXiv:1811.06743`, `doi:10.1007/JHEP02(2019)155`.

[89] F. Jegerlehner, Hadronic Contributions to Electroweak Parameter Shifts: A Detailed Analysis, Z. Phys. C32 (1986) 195. `doi:10.1007/BF01552495`.

[90] F. Jegerlehner, Electroweak effective couplings for future precision experiments, Nuovo Cim. C034S1 (2011) 31–40. `arXiv:1107.4683`, `doi:10.1393/ncc/i2011-11011-0`.

[91] A. Czarnecki, W. J. Marciano, Electroweak radiative corrections to polarized Møller scattering asymmetries, Phys. Rev. D53 (1996) 1066–1072. `arXiv:hep-ph/9507420`, `doi:10.1103/PhysRevD.53.1066`.

[92] A. Czarnecki, W. J. Marciano, Polarized Møller scattering asymmetries, Int. J. Mod. Phys. A15 (2000) 2365–2376. `arXiv:hep-ph/0003049`, `doi:10.1016/S0217-751X(00)00243-0, 10.1142/S0217751X00002433`.

[93] J. Erler, M. J. Ramsey-Musolf, The Weak mixing angle at low energies, Phys. Rev. D72 (2005) 073003. `arXiv:hep-ph/0409169`, `doi:10.1103/PhysRevD.72.073003`.

[94] J. Erler, R. Ferro-Hernández, Weak Mixing Angle in the Thomson Limit, JHEP 03 (2018) 196. `arXiv:1712.09146`, `doi:10.1007/JHEP03(2018)196`.

[95] D. Bernecker, H. B. Meyer, Vector Correlators in Lattice QCD: Methods and applications, Eur. Phys. J. A47 (2011) 148. `arXiv:1107.4388`, `doi:10.1140/epja/i2011-11148-6`.

[96] A. Francis, G. von Hippel, H. B. Meyer, F. Jegerlehner, Vector correlator and scale determination in lattice QCD, PoS LATTICE2013 (2013) 320. `arXiv:1312.0035`, `doi:10.22323/1.187.0320`.

[97] M. Cè, A. Gérardin, K. Ottnad, H. B. Meyer, The leading hadronic contribution to the running of the Weinberg angle using covariant coordinate-space methods, PoS LATTICE2018 (2018) 137. `arXiv:1811.08669`.

[98] F. Burger, K. Jansen, M. Petschlies, G. Pientka, Leading hadronic contributions to the running of the electroweak coupling constants from lattice QCD, JHEP 11 (2015) 215. `arXiv:1505.03283`, `doi:10.1007/JHEP11(2015)215`.